

1  
2  
3  
4  
5  
6  
7  
8  
9  
10  
11  
12  
13  
14  
15  
16  
17  
18  
19  
20  
21

**Tectonic position, structure, and Holocene activity of the Hofsjökull volcanic system,  
central Iceland**

**Ásta Rut Hjartardóttir\* and Páll Einarsson**

Ásta Rut Hjartardóttir  
Institute of Earth Sciences, University of Iceland  
Askja, Sturlugata 7, 101 Reykjavík, Iceland  
e-mail: [astahj@hi.is](mailto:astahj@hi.is)

Páll Einarsson  
Institute of Earth Sciences, University of Iceland  
Askja, Sturlugata 7, 101 Reykjavík, Iceland  
e-mail: [palli@hi.is](mailto:palli@hi.is)

\*Corresponding author

22 **Abstract**

23 The Hofsjökull volcanic system is located at the northern border of the Hreppar microplate on  
24 the Mid-Atlantic plate boundary in Iceland, between the more active Western and Eastern  
25 volcanic zones. In this study, fractures, and faults within the fissure swarms of the volcanic  
26 system were mapped and the throw and orientation of faults measured. This was done using  
27 both aerial photographs and ArcticDEM digital elevation models, as well as during fieldwork.  
28 The Hofsjökull volcanic system contains 3-4 fissure swarms extending northwards or  
29 southwards from the glacially covered Hofsjökull central volcano. Although these fissure  
30 swarms have been active during the Holocene, no clear sink holes were found along the faults,  
31 suggesting that they have been filled by sediments. This indicates that the fissure swarms have  
32 been less active than fissure swarms in other branches of the plate boundary in Iceland where  
33 GPS geodetic measurements show current spreading. Unbroken hyaloclastite covering a fault  
34 in the northern Hofsjökull fissure swarm suggests that this part of the northern Hofsjökull  
35 fissure swarm has not been active since the earliest part of Holocene, or during the latest stage  
36 of glaciation in the area. Still, the fault scarps in the northern Hofsjökull fissure swarm are  
37 rather sharp, indicating little erosion by glaciers. This may suggest increased activity in the  
38 Hofsjökull fissure swarm during the end of the last glaciation or at the beginning of the  
39 Holocene, which is in line with other studies showing increased magmatic activity in Iceland  
40 during that period. Fractured Holocene lava flows in the southern and western Hofsjökull  
41 fissure swarms indicate that they have been active during the Holocene. The Kerlingarfjöll  
42 rhyolitic massif is located south of the Hofsjökull central volcano. The southern fissure swarms  
43 are located both east and west of Kerlingarfjöll, but no clear indications are found of the fissure  
44 swarm in the rhyolitic massif itself. This may occur as dike intrusions (which likely form the  
45 faults) are prevented from penetrating the rhyolite due to density differences, and/or due to the  
46 topographic high of Kerlingarfjöll.

47

48 **Keywords:** rift zones, Iceland, fissure swarms, dikes, density barriers

49

50

51

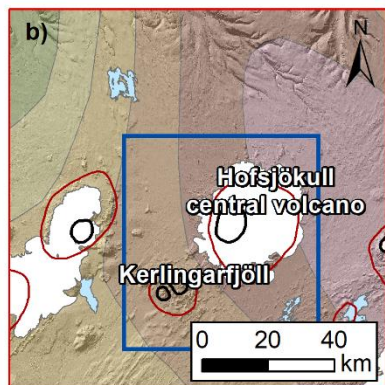
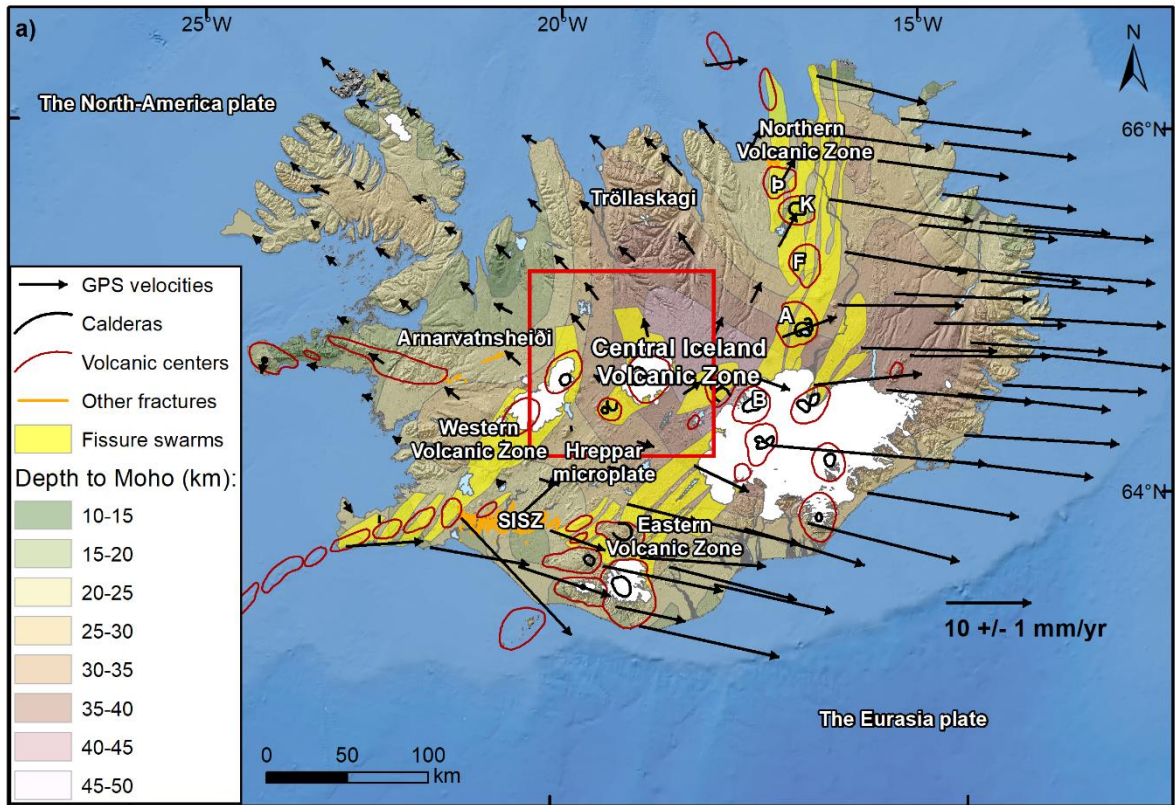
52

## 53 **1. Introduction**

54 The divergent segments of the plate boundary in Iceland are delineated by volcanic systems  
55 consisting of fissure swarms and central volcanoes (e.g. Einarsson, 2008; Sæmundsson,  
56 1978). The fissure swarms radiate from the central volcanoes and consist of normal faults,  
57 open fissures, and eruptive fissures that are near-perpendicular to the local direction of  
58 spreading. They are defined as an area with a high density of faults and/or fissures, whereas  
59 their surroundings have few or no faults or fissures at all. These fissure swarms seem to be  
60 formed and reactivated during dike intrusions, which cause fault movements above the dike  
61 (Pollard et al., 1983; Rubin and Pollard, 1988; Sigurdsson, 1980). Sometimes the dikes reach  
62 the surface as fissure eruptions (Hjartardóttir et al., 2016b). The central volcanoes are  
63 typically basaltic, but with a component of silicic products. Many of them have caldera  
64 structures and an active geothermal system. The Hofsjökull volcanic system in Central  
65 Iceland has all these typical characteristics of the plate boundary systems, and yet it is located  
66 outside the currently most active segments of the plate boundary (Árnadóttir et al., 2009;  
67 Sigmundsson et al., 2020). It is located on the northern boundary of the Hreppar Microplate  
68 that was created by the shift in spreading in the southern part of Iceland from the Western  
69 Volcanic Zone (WVZ) to the Eastern Volcanic Zone (EVZ) (Fig. 1). This shift began about 3  
70 Ma and is still in progress. The microplate was separated from the Eurasia plate by the  
71 propagating EVZ but has not fully been attached to the North America Plate. The spreading  
72 rate across the WVZ is about 4-5 mm/year near the Hengill triple junction and decreased  
73 northwards to almost zero at its northern end (Fig. 1) (LaFemina et al., 2005). Conversely,  
74 spreading rate across the EVZ increases northwards, from about 11 mm/year in the southwest  
75 to ~19 mm/year in the northeast (LaFemina et al., 2005). The pole of relative rotation of the  
76 microplate with respect to North America must therefore be near the northern end of the WVZ  
77 (Einarsson, 2008), so the relative plate velocity across the northern boundary of the  
78 microplate must be small, and possibly compressive in a N-S direction. This low velocity is  
79 consistent with low seismicity of the area. The Hofsjökull system, however, appears to  
80 contradict this simplified picture, as it would imply small or no divergent stresses along the  
81 Hofsjökull volcanic system. Both the central volcano and the fissure swarms are rather  
82 impressive structures, the former has a prominent caldera, and the latter have large-offset  
83 normal faults. In addition, the fissure swarms extend into the plates on both sides of the  
84 boundary and do not follow its trend. An added complication to the structural picture is  
85 presented by the Kerlingarfjöll central volcano that is located within the southern fissure

86 swarms of Hofsjökull and is frequently taken to be a part of the Hofsjökull system. It has  
87 high proportion of rhyolitic products, and appears to have two buried calderas (Hjartarson et  
88 al., 2019). The local stress field of the Kerlingarfjöll central volcano could thus have  
89 influenced the southern Hofsjökull fissure swarms.

90 In this paper we try to clarify the structural position of the Hofsjökull volcanic system within  
91 the plate tectonic framework of Iceland. We find the extent of the Hofsjökull fissure swarms,  
92 their width and length by mapping fractures and delineating the outlines of those fractured  
93 areas. By measuring the throws of faults, we estimate the widening across the fissure swarms,  
94 also in the northern Hofsjökull fissure swarm which propagates into the North American  
95 plate. Various geological data, such as lava flows of a known age and information on glacial  
96 moraines, is used to acquire time constraints on the activity of the faults and fractures within  
97 the fissure swarms. The interaction between the Hofsjökull fissure swarms and the  
98 Kerlingarfjöll rhyolitic massif will also be discussed, especially the influence of density  
99 differences on the propagation of shallow dike intrusions and eruptions. By doing this, the  
100 aim is to shed a light on how this volcanic system at the periphery of the active plate  
101 boundary works.



102

103 Fig. 1. a) Overview of the plate boundary in Iceland. Outlines of fissure swarms, calderas and  
 104 volcanic centers delineate the plate boundaries, they are modified from Einarsson and

105 Sæmundsson (1987). The GPS vectors, spanning the time between 1993 and 2004, are from  
106 Árnadóttir et al. (2009) and Valsson et al. (2007). Information about the depth to the Moho  
107 (indicating crustal thickness) is from Brandsdóttir and Menke (2008). The black arrow at the  
108 lower right corner shows the scale of the vectors. The red frame indicates the location of Fig.  
109 1b. Information on other fractures are from Hjartardóttir et al. (2016a); Hjartardóttir et al.  
110 (2016c); and Magnúsdóttir and Brandsdóttir (2011). Cartographic data are from the IS50  
111 database of the National Land Survey of Iceland. P=Peistareykir, K=Krafla, F=Fremrinámar,  
112 A=Askja, B=Bárðarbunga b) The Central Iceland Volcanic Zone. The blue frame indicates the  
113 location of Fig. 1c. c) A geological map of the Hofsjökull fissure swarm, data on bedrock  
114 geology are from Iceland Geosurvey (ÍSOR) (Hjartarson et al., 2019), the fractures were  
115 mapped by the authors of this paper.

116

## 117 **2. Rifting events and episodes**

118 Observations in Iceland during the last several decades have shown that most parts of the  
119 divergent plate boundaries are seismically inactive most of the time (Einarsson, 1991;  
120 Einarsson and Brandsdóttir, 2021; Jakobsdóttir, 2008). Large scale rifting has been observed  
121 twice in the last half century, during the Krafla rifting episode in 1975-1984 and Bárðarbunga  
122 dike injection and caldera collapse of 2014 (e.g. Dumont et al., 2018; Hjartardóttir et al.,  
123 2016b; Sigmundsson et al., 2015; Tryggvason, 1984). In both cases the rifting occurred along  
124 the fissure swarms of these volcanoes and the extension during the rifting was of the order of  
125 5-8 m. During the time between such episodes the relative plate movements is taken up by  
126 aseismic deformation and stretching of the plate margins. Fissure swarms within the main  
127 plate boundary zones in Iceland appear to develop and deform in response to diking, while  
128 having little or no deformation during other times. During such rifting episodes, grabens  
129 above the propagating dikes subside. The subsidence is often around 1-6 m and is mostly  
130 taken up by the boundary faults of the graben (Hjartardóttir et al., 2016b; Saemundsson, 1992;  
131 Sigurdsson, 1980). Similar behavior has also been seen in rift zones in east Africa (e.g.  
132 Wright et al., 2006). The lack of non-magmatic fault movements has been suggested to be  
133 because it takes a long time before deviatoric stresses due to crustal movements alone build  
134 up to a level of reactivation. However, when magma is available, a dike intrusion can release  
135 the accumulated crustal stresses long before they would have been released if no magma was  
136 available (Sigmundsson, 2006). It has, however, been unclear whether and how such

137 processes occur in the less active parts of the plate boundary in Iceland, such as in the  
138 Hofsjökull fissure swarm.

139

### 140 **3. Geological settings**

141 The fissure swarms extend at least 40 km to the north and 30 km to the south of the Hofsjökull  
142 central volcano (Einarsson and Sæmundsson, 1987) (Fig. 1a). The southern fissure swarm  
143 extends into the heavily faulted Hreppar microplate (Khodayar et al., 2020). Radio echo-  
144 soundings on the glacier show that the Hofsjökull central volcano has a 6 - 7 km wide and ~600  
145 m deep caldera, which is covered by the Hofsjökull glacier (Björnsson, 1986; 1988). Despite  
146 the large caldera, no ash layers from the Holocene epoch have been associated with the  
147 Hofsjökull central volcano. It is nevertheless possible that several basaltic tephtras of unknown  
148 origin, found in soil profiles around the Vatnajökull glacier, are from the Hofsjökull central  
149 volcano (Óladóttir et al., 2011). Most of the source vents of these postglacial lava flows are  
150 now beneath the Hofsjökull glacier and therefore not visible. The few source vents that can be  
151 seen are located so close to the glacier that it is not possible to determine whether they are  
152 individual vents or a part of an eruptive fissure. It has been poorly understood how often this  
153 volcano is activated and how far dikes have propagated in the fissure swarms. The uncertainty  
154 of the behavior of the Hofsjökull fissure swarm is further reinforced by its unique location  
155 between the Western Volcanic Zone and the Eastern and Northern Volcanic Zones. There are  
156 therefore no other fissure swarms in similar settings to which the activity of the Hofsjökull  
157 fissure swarm has a resemblance. Despite the low activity of the Hofsjökull central volcano, it  
158 is not completely inactive. In the summer of 2013, a jökulhlaup flood with sulfuric smell  
159 originated from the Hofsjökull glacier. Although earthquakes were not detected during this  
160 event, a new ice cauldron was found within the glacier after the flood, on the caldera boundary  
161 (Fig. 1). This suggests that there is a high-temperature geothermal area within the volcano.  
162 Geothermal areas are also found in the area north of the northern Hofsjökull fissure swarm  
163 (Torfason, 2003).

164 The age of the bedrock of the Hofsjökull fissure swarm increases with distance from the  
165 Hofsjökull central volcano (Jóhannesson and Sæmundsson, 1998a). A few unglaciated lava  
166 flows have been found around the glacier (Fig. 1) (Hjartarson et al., 2019; Jóhannesson and  
167 Sæmundsson, 1998b). The youngest lava flows are 3000-4500 years old, located just north of  
168 the Hofsjökull glacier (Fig. 1c) (Hjartarson et al., 2019). Several 4500-7000 years old lava flows

169 are located in the southern Hofsjökull fissure swarm, close to the Hofsjökull glacier and early  
170 Holocene lava flows (>7000 years old) can be found east and west of the Hofsjökull glacier. In  
171 addition, the western Hofsjökull fissure swarm cuts the ~10.000 years old Kjalhraun lava (Fig.  
172 1c) (Eason et al., 2015; Hjartarson et al., 2019). These postglacial lava flows are all found close  
173 to the Hofsjökull central volcano, with sources beneath or close to the edge of the glacier.  
174 Similarly, mafic hyaloclastite, less than 0,8 Ma old, is mostly found close to the central volcano  
175 (Hjartarson et al., 2019). Some of the hyaloclastite is from the Weichselian period, from  
176 ~10.000 to ~110.000 years old (Helmens, 2014). The youngest hyaloclastite is mostly located  
177 at the northwestern margin of the Hofsjökull glacier, although small patches of the youngest  
178 hyaloclastite can be found southwest of Hofsjökull (Fig. 1c) (Hjartarson et al., 2019). Basaltic  
179 and intermediate interglacial and supraglacial lavas and sediments of less than 0,8 Ma age can  
180 be found in up to ca 20 km distance north and south of the Hofsjökull glacier (Jóhannesson and  
181 Sæmundsson, 1998a). Both the southern and the northern Hofsjökull fissure swarms extend  
182 into basaltic and intermediate extrusive rocks and sediments of lower Pleistocene age (0,8-2,6  
183 Ma) (Jóhannesson and Sæmundsson, 1998a).

184 The Kerlingarfjöll volcanic center is sometimes considered to be a part of the Hofsjökull  
185 volcanic system (Fig. 1). It is characterized by rhyolitic, intermediate and basaltic formations,  
186 generally formed subglacially (Flude et al., 2010; Grönvold, 1972; Stevenson et al., 2009), and  
187 altered by high-temperature geothermal activity (Torfason, 2003). The dating of rocks in  
188 Kerlingarfjöll indicates that the age of rocks there ranges approximately between 68.000 and  
189 350.000 years (Flude et al., 2010). Two calderas have been identified within the area  
190 (Hjartarson et al., 2019).

191

#### 192 **4. Methods**

193 The fractures and faults in the Hofsjökull fissure swarms were mapped in detail from aerial  
194 photographs from Loftmyndir Inc. These features appear to be mostly dilatational, since en-  
195 echelon arrangements, suggesting strike-slip faulting, are lacking. Eruptive fissures are also  
196 almost non-existent, most of them are buried under the Hofsjökull glacier. The ArcticDEM  
197 Digital Elevation Models (Porter et al., 2018) were used to improve the mapping of the faults.

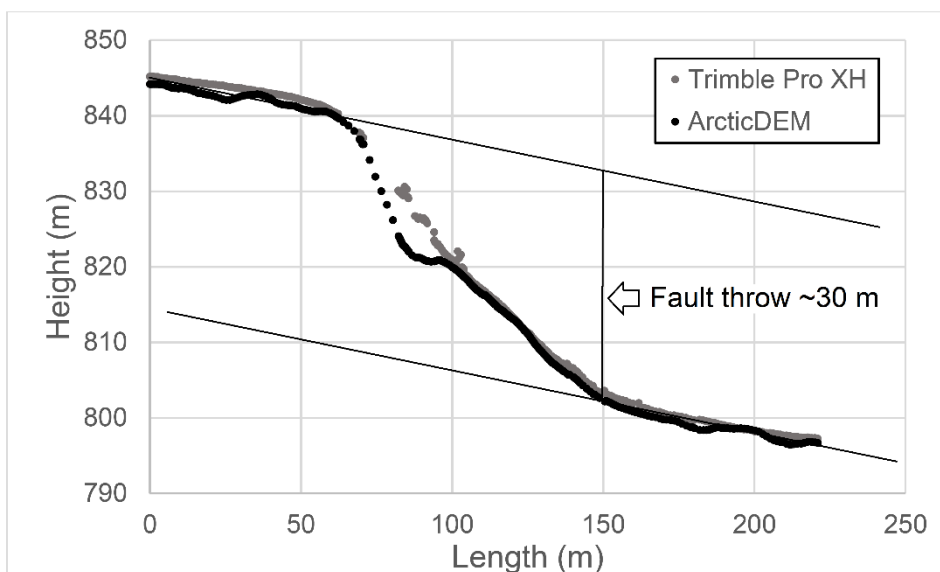
198 The ArcticDEM was also used to study throws of faults and to make cross-sections of  
199 the grabens in the Hofsjökull fissure swarms, in a similar manner as has been done in the  
200 Western Volcanic Zone, Iceland (Hjartardóttir et al., 2016a; 2015). In the Western Hofsjökull



201 fissure swarm, an ArcticDEM from 3<sup>rd</sup> of November 2013 and 3<sup>rd</sup> of November 2014 was used  
202 for this purpose.

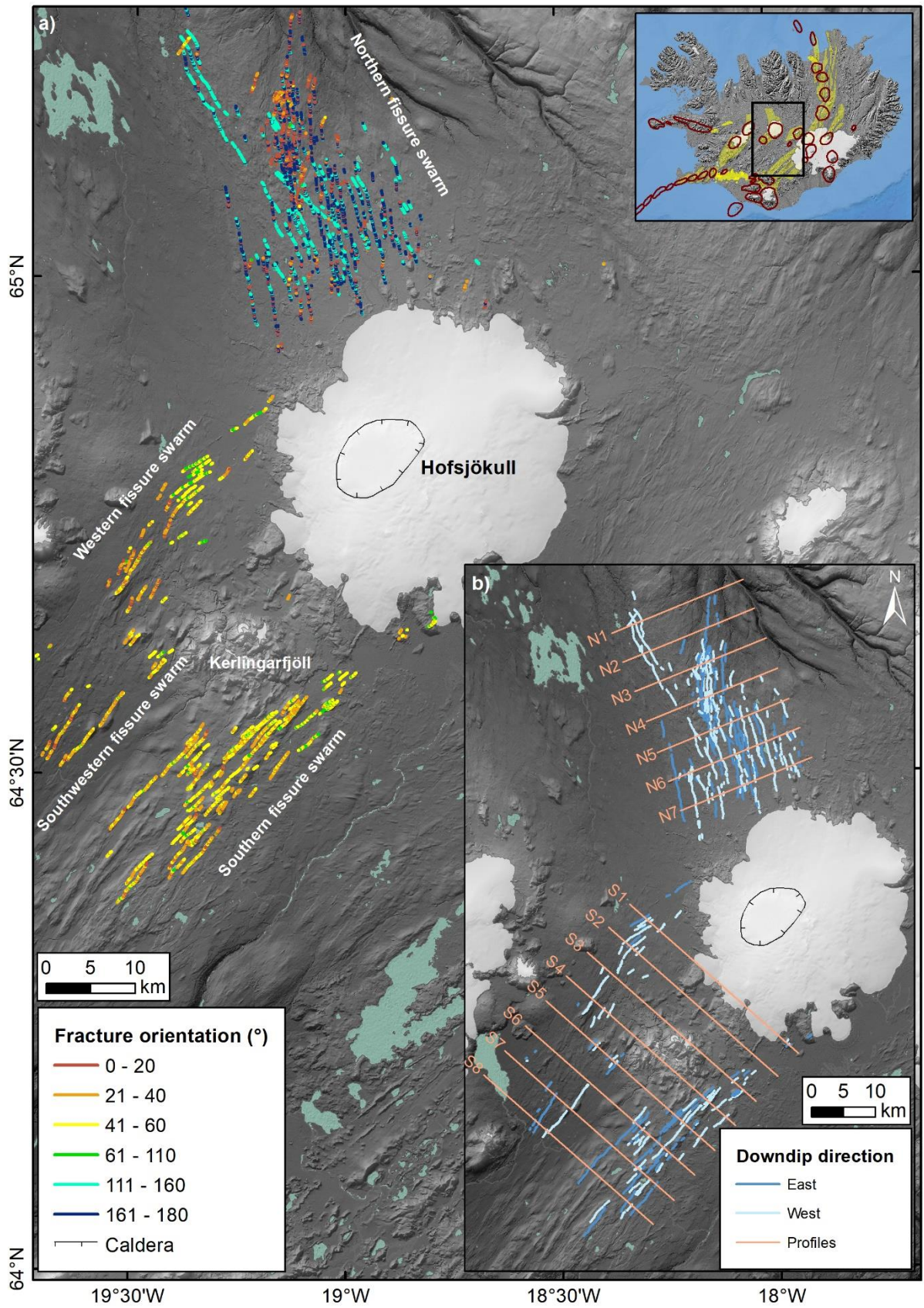
203 The cross-sections were made by using the 3D Analyst tool in ArcMap. Each profile is  
204 measured perpendicular to the fault and profiles are measured with 200 m interval along the  
205 faults. The profiles were long enough so that the general topography could be measured and  
206 taken into account (see as an example the gently sloping topography at the beginning and end  
207 of the profile in Fig. 2). The throws of faults were measured from the profiles and the results  
208 registered into a point shapefile where the profile was taken. The points were then colored  
209 according to the throw of the fault.

210 Field work was done within the Hofsjökull fissure swarms in the summers of 2019 and  
211 2020. The purpose of the field work was ground truthing. The throws of faults were measured  
212 by using Trimble ProXH and Trimble Pathfinder ProXR Differential GPS equipments. These  
213 profiles were then compared to the ones made by the ArcticDEM. The difference between these  
214 two methods is negligible (e.g. Fig. 2), and therefore it was concluded that the ArcticDEM  
215 could be used for this purpose.



216

217 Fig. 2. An example of a comparison between a profile measured in the field with a Trimble  
218 ProXH GPS instrument and a profile measured from the ArcticDEM. The figure also shows  
219 how the throw of faults is measured. This profile is taken in the southern HFS. As can be seen  
220 from the graph, the relative height differences between these two methods is negligible.



221

222 Fig. 3. a) Different segments of the Hofsjökull fissure swarm. Faults are colored according to

223 their orientations. b) The downdip direction of faults. The location of profiles in Figs. 7 and 15

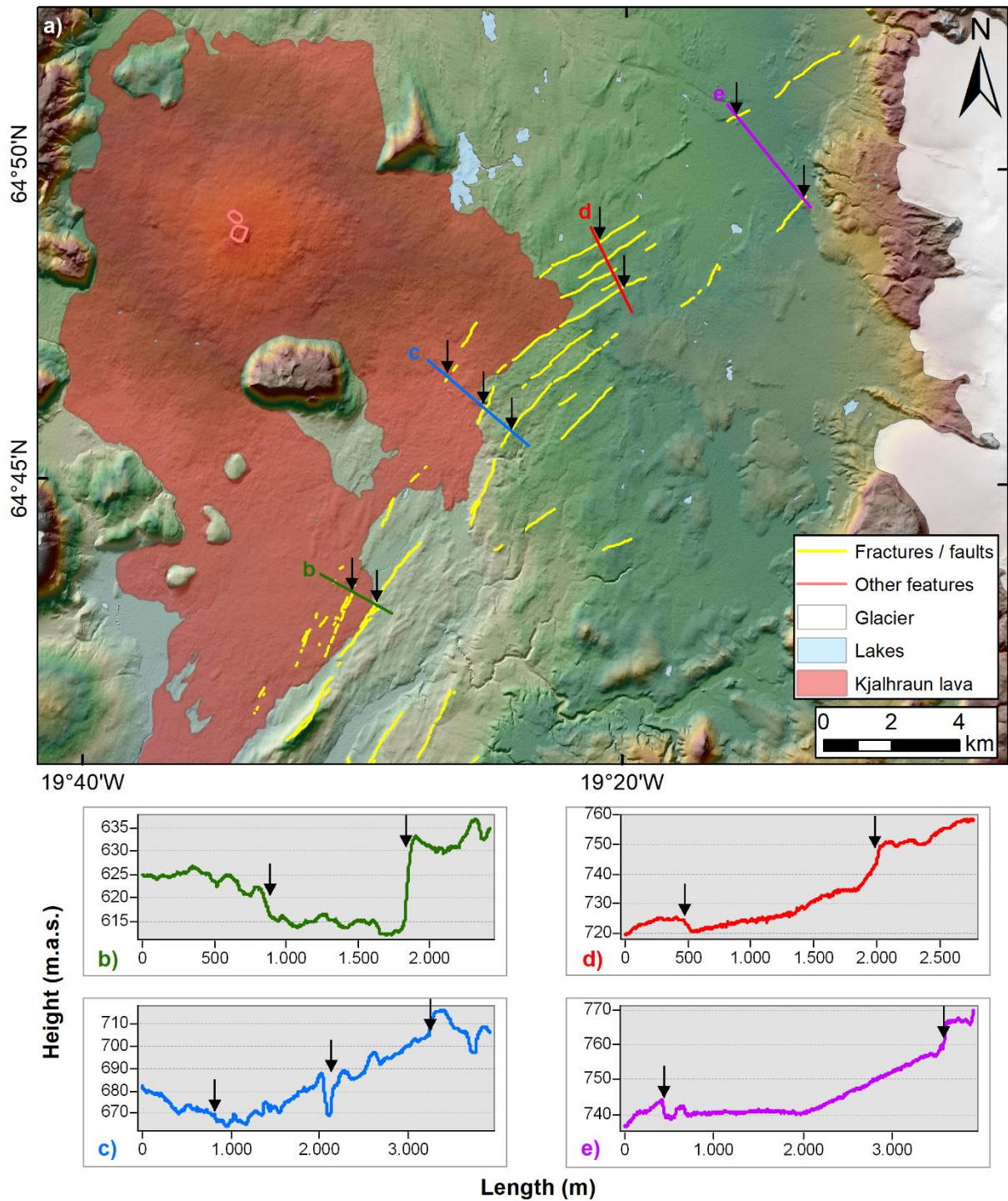
224 are shown. The digital elevation model in the background is from TanDEM-X, from the  
225 German Space Agency. Outlines of glaciers, rivers and lakes are from the IS50 database of the  
226 National Land Survey of Iceland.

227

## 228 **5. Results**

229 The Hofsjökull volcanic system has three to four fissure swarms, two to three extending to the  
230 south, and one extending to the north. In addition, Holocene volcanic eruptions have taken place  
231 at several places around the Hofsjökull glacier. The lava flows are visible although most of  
232 their eruptive vents have been obliterated by the glacier. Each of the fissure swarms has its own  
233 characteristics, they have different orientations, width, and extent (Fig. 3).

234



235

236 Fig. 4. The western Hofsjökull fissure swarm. a) The fissure swarm cuts the postglacial  
 237 Kjalhraun lava. b)-e) Profiles across the fissure swarm. The location of the profiles is shown in  
 238 a). The extent of the Kjalhraun lava is from Sinton et al. (2005). ArcticDEM courtesy of the  
 239 Polar Geospatial Center.

240

241

242 **5.1. The western Hofsjökull fissure swarm:**

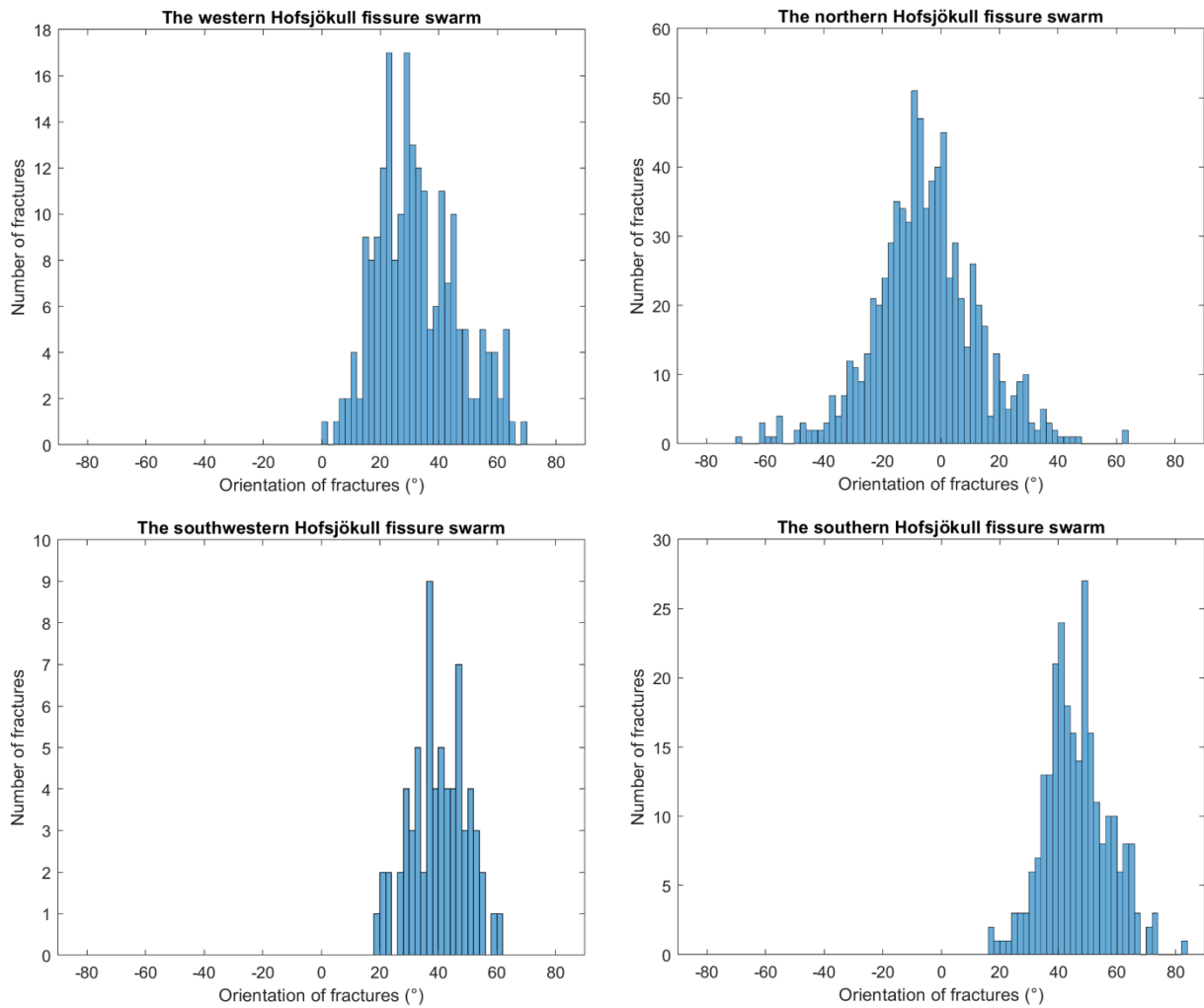
243 The western Hofsjökull fissure swarm extends from the western part of the Hofsjökull glacier.  
244 Its general direction is towards NNE, most commonly striking around 20-30°N. However,  
245 closest to the glacier, the fissure swarm gradually changes direction and is oriented more  
246 towards the NE, often striking 40-60°N (Figs. 3-5). Therefore, the fissure swarm appears to  
247 radiate away from the volcano beneath the glacier.

248 The length of the Western Hofsjökull fissure swarm is rather uncertain. It is at least ~30  
249 km long, but fractures can be found to up to 40 km distance. The fissure swarm extends into  
250 the Hreppar microplate, where it merges with older fractures and faults. In addition, there is  
251 another fissure swarm slightly to the east of this one, extending towards the south from the  
252 western end of Kerlingarfjöll (Fig. 3, the southwestern fissure swarm). This fissure swarm is  
253 possibly the same one as the western Hofsjökull fissure swarm, but it could also be a separate  
254 entity and will therefore be described separately.

255 The western Hofsjökull fissure swarm is rather narrow, mostly about 6 km wide. It cuts  
256 the Kjalhraun lava, which is postglacial and has been estimated to be ~10.000 years old (Eason  
257 et al., 2015; Hjartarson et al., 2019). The throws of fractures and faults within the Kjalhraun  
258 lava are very little, on average only around 0.5 m, these are mostly tensional fractures (e.g. Fig.  
259 4a and 4c). The older surface formations generally have greater offset (e.g. Fig. 4b), although  
260 the throw of faults in the northern part of the Western Hofsjökull fissure swarm is generally  
261 less than 10 m (Fig. 6).

262 Transects across the Western Hofsjökull fissure swarm indicate that it only consists of  
263 one graben (Figs. 4 and 7). The graben is about 1.5 km wide in the southern part (Fig. 4b, 4c  
264 and 4d), but about 3 km wide in the northernmost part (Fig. 4e).

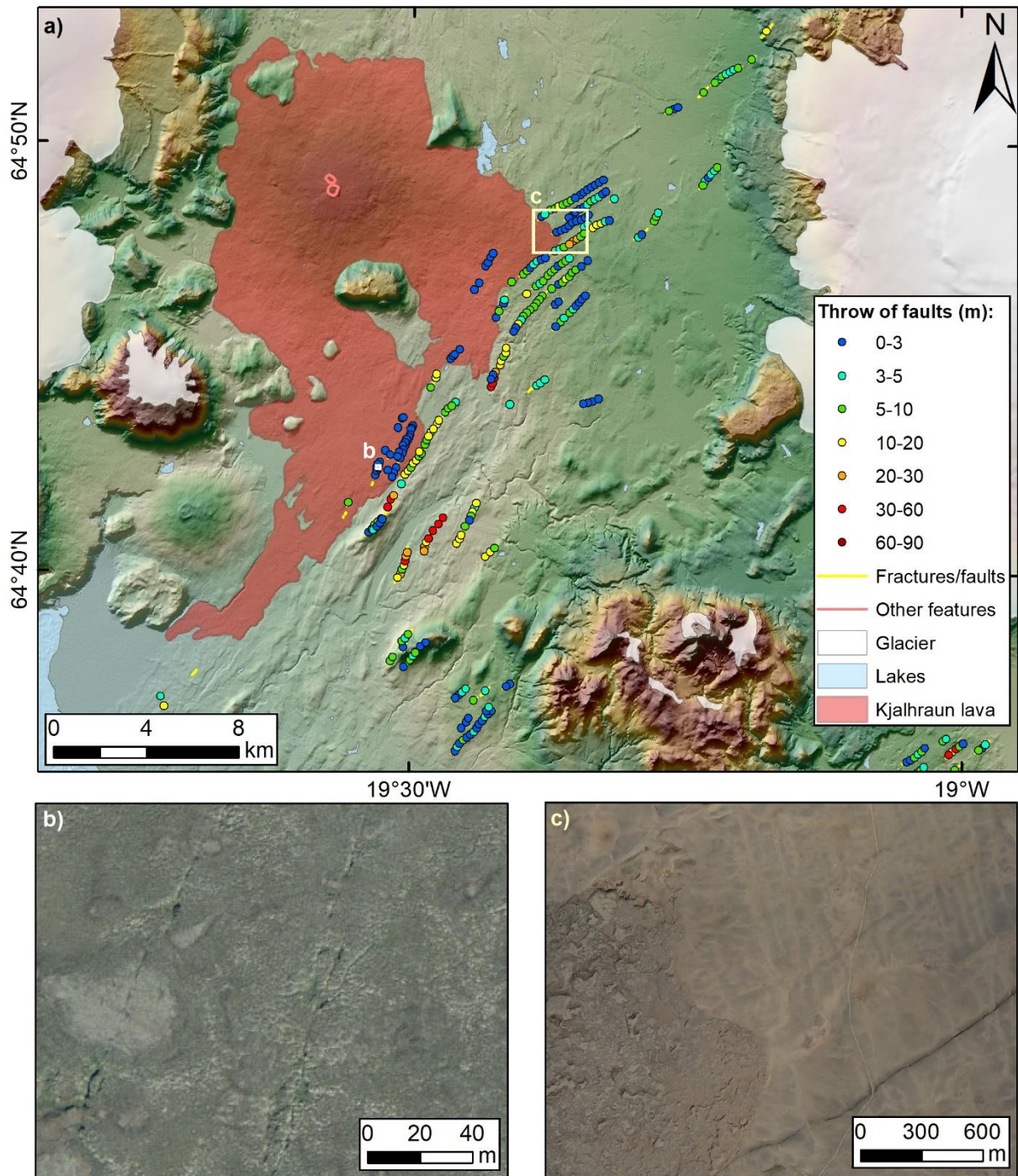
265



266

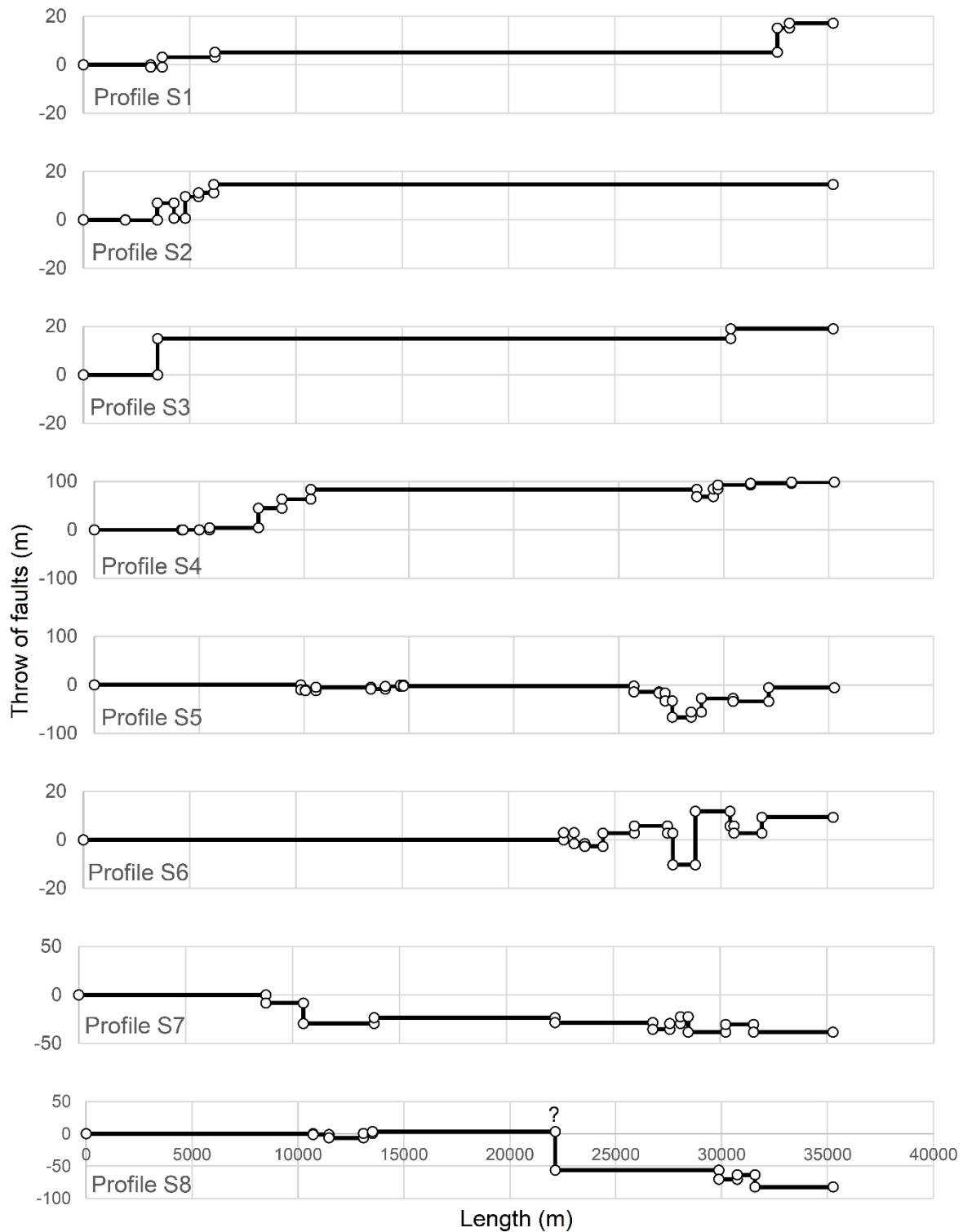
267 Fig. 5. Orientation of fractures in different fissure swarms of the Hofsjökull volcanic system.  
 268 The orientation is represented in degrees from north, positive numbers indicating northeasterly  
 269 orientation, negative numbers representing northwesterly orientations.

270



271

272 Fig. 6. a) Throw of faults in the western Hofsjökull fissure swarm. b) Aerial photograph  
 273 showing fractures in the postglacial Kjalhraun lava. c) Faults at the boundary of the postglacial  
 274 Kjalhraun lava and older formations, the location of the aerial photographs is shown in a). The  
 275 aerial photographs are from Loftmyndir Corp. The extent of the Kjalhraun lava is from Sinton  
 276 et al. (2005). ArcticDEM courtesy of the Polar Geospatial Center.



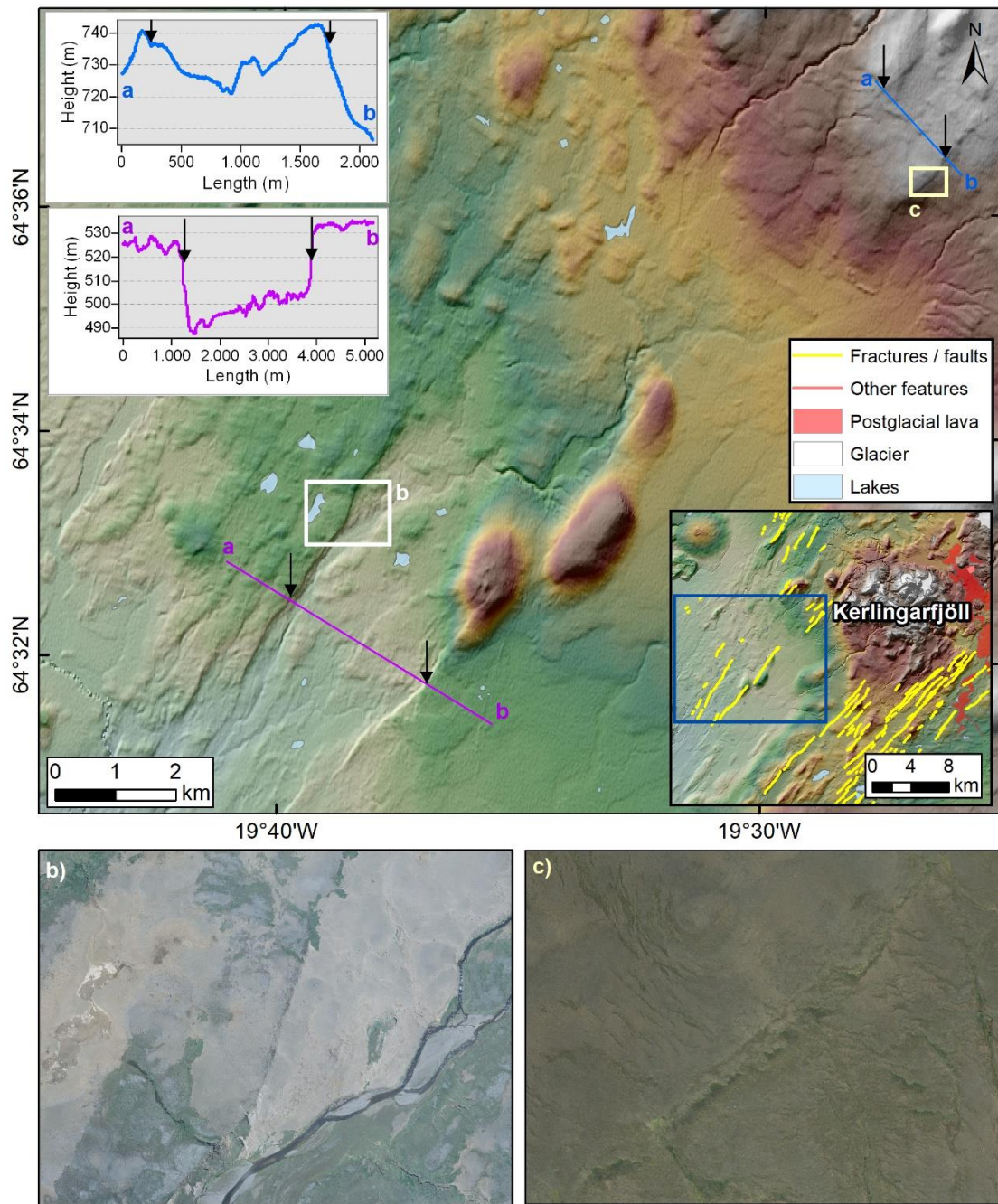
277

278 Fig. 7. Throw as a function of a distance along a profile across the southern Hofsjökull fissure  
 279 swarms, showing offset of faults. Negative values indicate downthrow towards the east. The  
 280 location of the profiles is shown in Fig. 3.

281

282





283

284 Fig. 8. a) The southwestern Hofsjökull fissure swarm. Inset graphs show profiles across  
 285 different parts of the fissure swarm. ArcticDEM courtesy of the Polar Geospatial Center. Note  
 286 the generally small throws of faults close to Kerlingarfjöll (blue profile), whereas the fault  
 287 throws increase towards the south (e.g. purple profile). b) Aerial photograph from the  
 288 Loftmyndir Corp. showing a fault in the southern part of the southwestern Hofsjökull fissure  
 289 swarm, c) Aerial photograph showing a fault in the northern part of the fissure swarm. The  
 290 locations of the aerial photographs are shown in a).

291

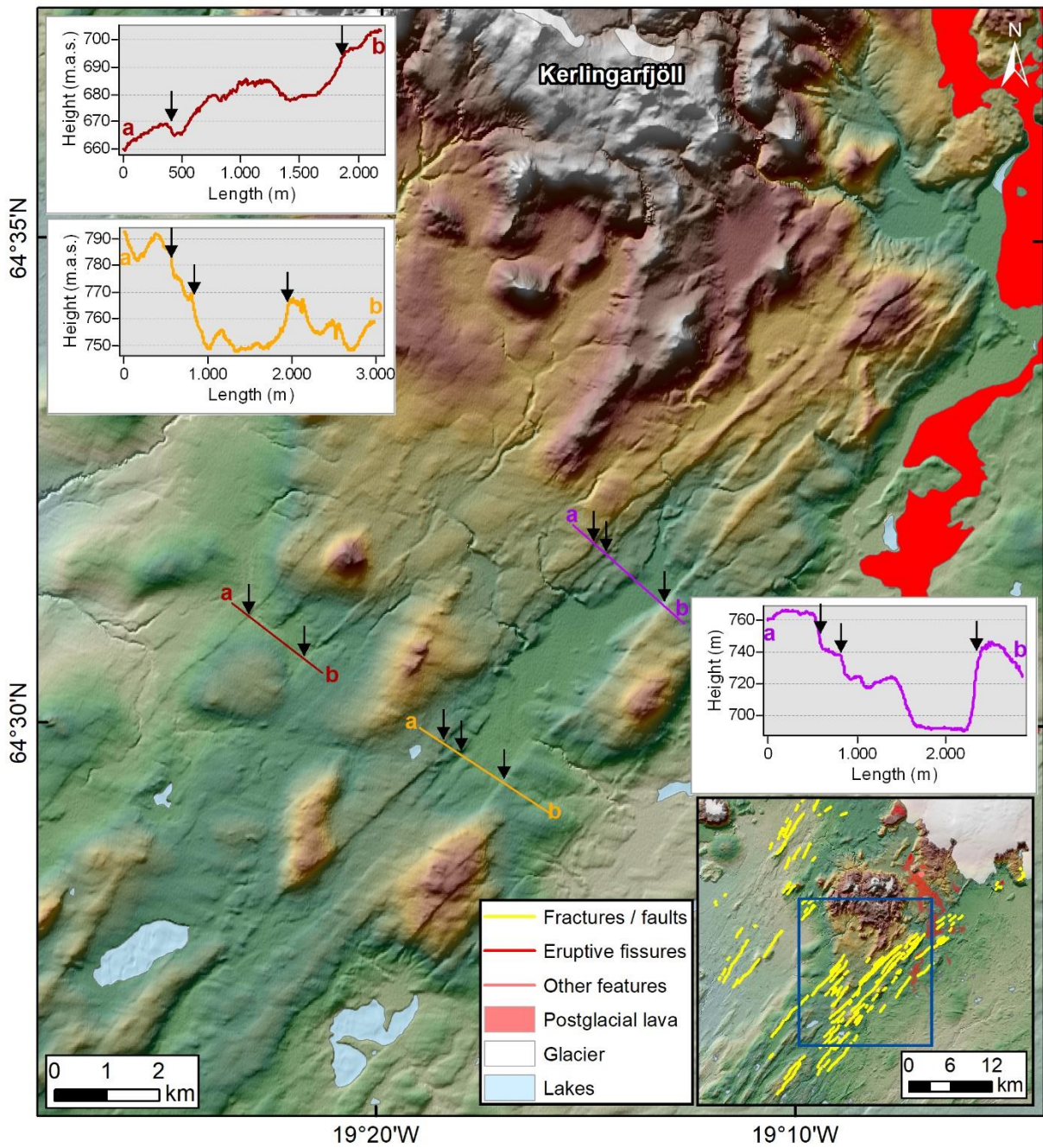
292

293 **5.2. The southwestern Hofsjökull fissure swarm**

294 This part of the Hofsjökull fissure swarm could be the southern part of the western fissure  
295 swarm, but it could also be a separate entity and will therefore be described separately.

296 The southwestern Hofsjökull fissure swarm is located to the west and south of the  
297 Kerlingarfjöll massif. Near Kerlingarfjöll, the throws of the faults are small (often less than 3.5  
298 m). Towards the south, the throws increase significantly, and can sometimes be more than 30  
299 m (Figs. 7 and 8). This fissure swarm has one clear graben which is about 3 km wide in the  
300 northern part (e.g. Fig. 8, purple profile), but gets narrower towards the south, where it is about  
301 2 km wide. The faults in this fissure swarm trend towards the NE, with the most common trends  
302 between 30 and 50° N (Fig. 5).

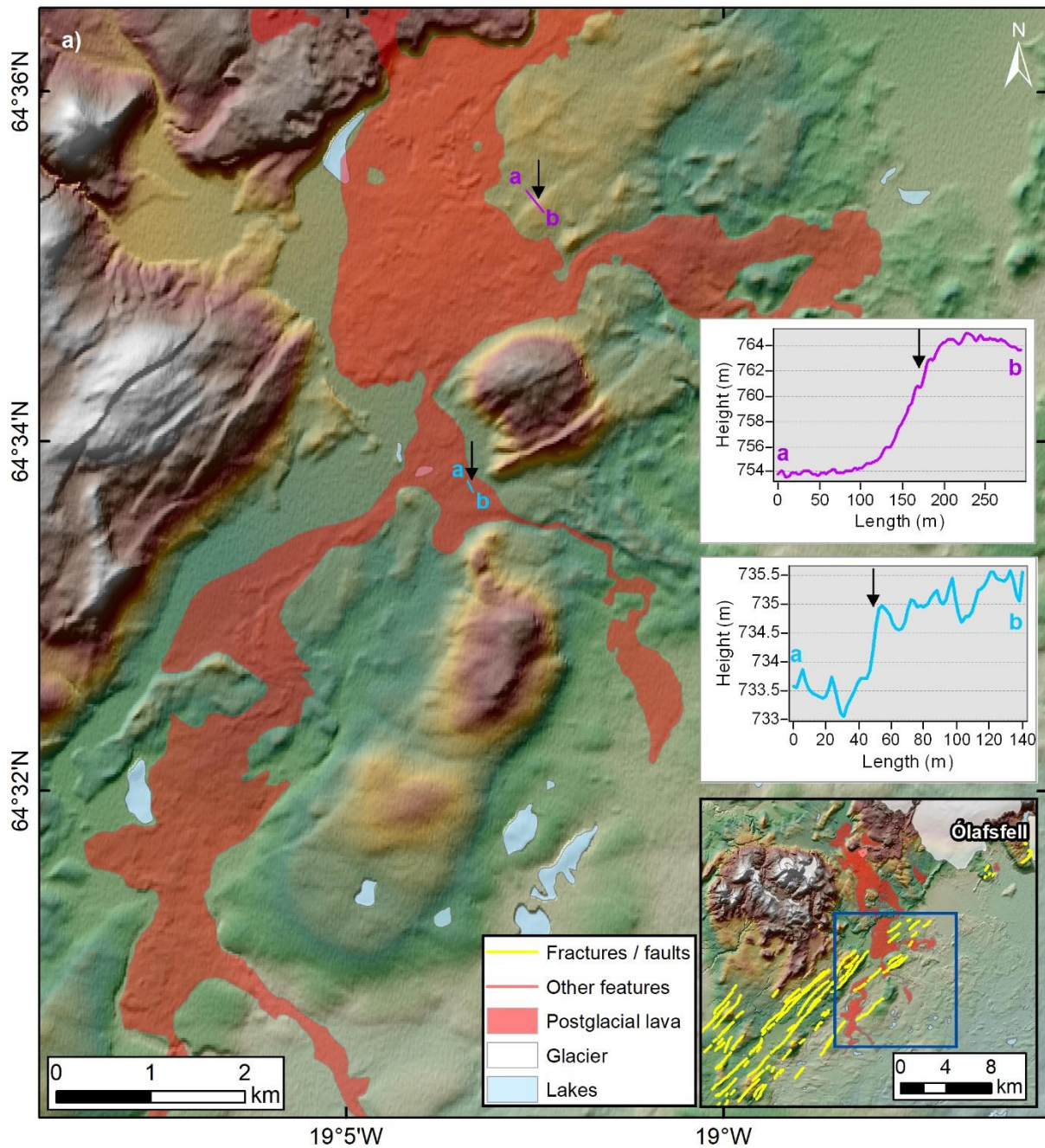
303



304

305 Fig. 9. The southern Hofsjökull fissure swarm. Inset graphs show profiles across different  
 306 grabens in the fissure swarm. Outline of the postglacial lava is from Hjartarson et al. (2019).  
 307 ArcticDEM courtesy of the Polar Geospatial Center.

308



309

310 Fig. 10. The southern Hofsjökull fissure swarm. Here, the fissure swarm cuts the postglacial  
 311 Illahraun lava. Inset graphs show profiles across different parts of the fissure swarm. The purple  
 312 profile shows a fault with a throw of about 10 m, whereas the light-blue profile, which crosses  
 313 a fault in the postglacial Illahraun lava, shows very little throw (~1.5 m). Outline of the  
 314 postglacial lava is from Hjartarson et al. (2019). ArcticDEM courtesy of the Polar Geospatial  
 315 Center.

316

317

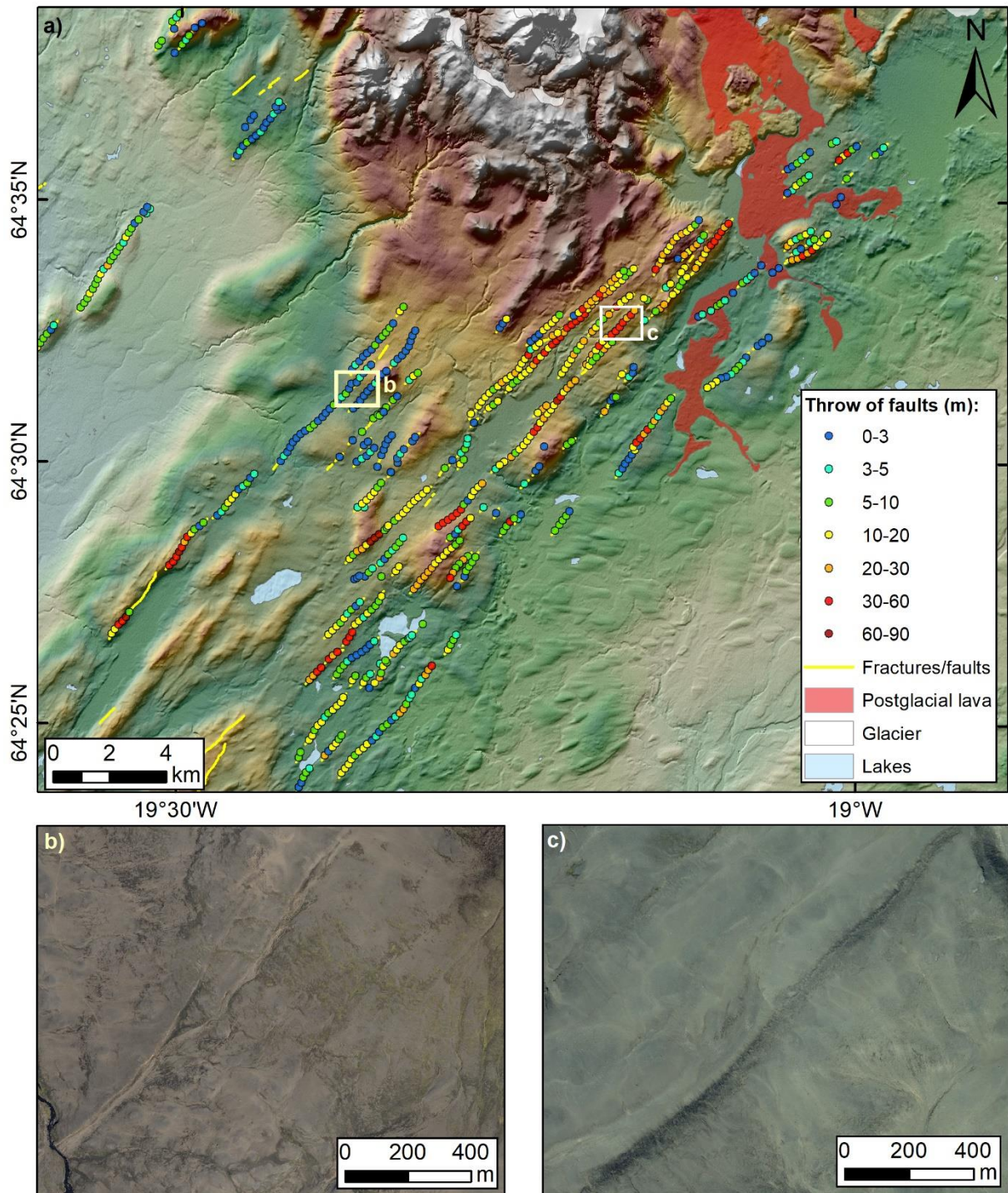
318

319 **5.3. The southern Hofsjökull fissure swarm:**

320 The southern Hofsjökull fissure swarm is about 50 km long. Its southern end is slightly  
321 uncertain since it merges with the highly fractured Hreppar microplate. Since the Hofsjökull  
322 fissure swarms are characterized by grabens we define the southern boundary of the fissure  
323 swarm to be where the clear graben structures end. The fissure swarm is up to 9 km wide and  
324 consists of several nearly parallel grabens, which can be up to ~2 km wide (Figs. 9 and 10). In  
325 some instances, grabens can be found within other grabens. The northeastern end of this fissure  
326 swarm starts near the Ólafsfell mountain (Fig. 10), but the start of the southwestern end of it is  
327 more uncertain. An eruptive fissure (which formed the Illahraun lava) is found north of  
328 Kerlingarfjöll, and is a part of this fissure swarm, but no fractures could be found in the  
329 Kerlingarfjöll massif. Few clear fractures are found north of Kerlingarfjöll, although there are  
330 some indications of eroded WNW-ESE lineaments which could be old fractures. However,  
331 some fractures are found south of Kerlingarfjöll (Fig. 9, e.g., dark red profile). No sink holes  
332 were found in the southern Hofsjökull fissure swarm, indicating that the fissure swarm has not  
333 been active recently, and that all sink holes have been filled with sediments. This differs from  
334 fissure swarms at volcanic systems which are located closer or at the main plate boundary in  
335 Iceland. Open sink holes along faults in loose sediments can, as an example, be seen in the  
336 nearby Tungnafellsjökull fissure swarm, as well as in the Krafla fissure swarm (Björnsdóttir  
337 and Einarsson, 2013; Hjartardóttir et al., 2012).

338 Faults in the southern Hofsjökull fissure swarm generally trend towards the NE, most  
339 commonly around 40-50°N (Fig. 5). This is a similar trend as is seen in the fissure swarm to  
340 the west of it, the southwestern fissure swarm, although the southern fissure swarm has more  
341 faults trending more eastwards (60-80°N) than the southwestern fissure swarm (Fig. 5).

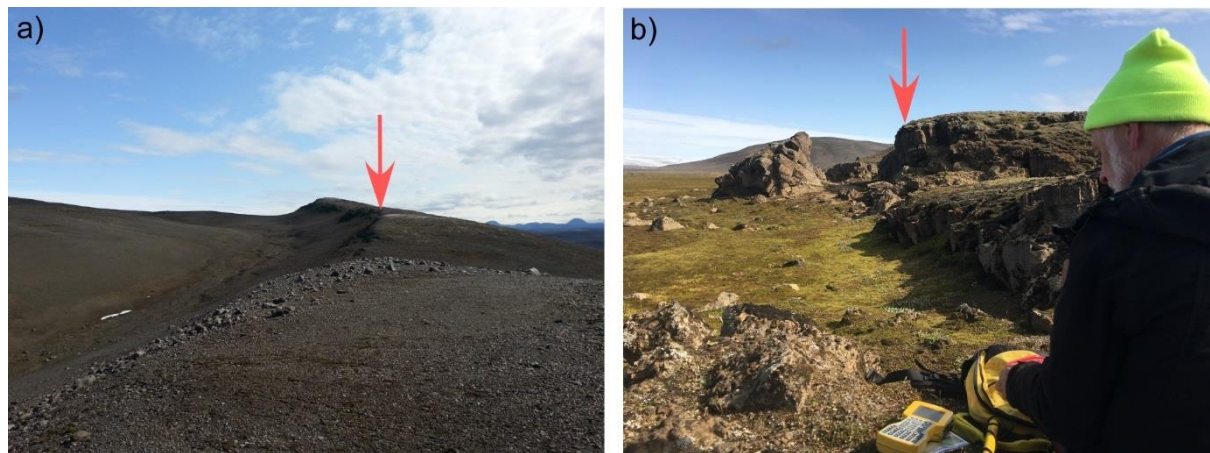
342 The throws of the boundary faults of the grabens in the southern Hofsjökull fissure  
343 swarm vary significantly (Figs. 7, 9 and 10). They are greatest in the main southern fissure  
344 swarm, where the throws of faults often reach 18-30 m (Figs. 11 and 12a). However, the throw  
345 of fractures just south of Kerlingarfjöll is much less, typically less than 10 m, and often less  
346 than 3.5 m (Fig. 11). This occurs even though these fractures are in surface formations of  
347 similar age as the fractures with the greater offsets to the east of them (Fig. 1c) (Hjartarson et  
348 al., 2019). The fractures in and around the postglacially formed Illahraun lava also often have  
349 little throws (1-2 m, Figs. 10-12b).



350

351 Fig. 11. a) Throws of faults in the southern Hofsjökull fissure swarm. Here, throws of faults are  
 352 generally larger at lower altitudes, whereas few faults are found at the topographically high  
 353 Kerlingarfjöll massif. Throws of faults are smaller directly south of Kerlingarfjöll, than of the  
 354 faults that cross the area east of Kerlingarfjöll. b) and c) Aerial photographs of selected areas,  
 355 locations shown in a). The aerial photographs are from Loftmyndir Corp. Outline of the

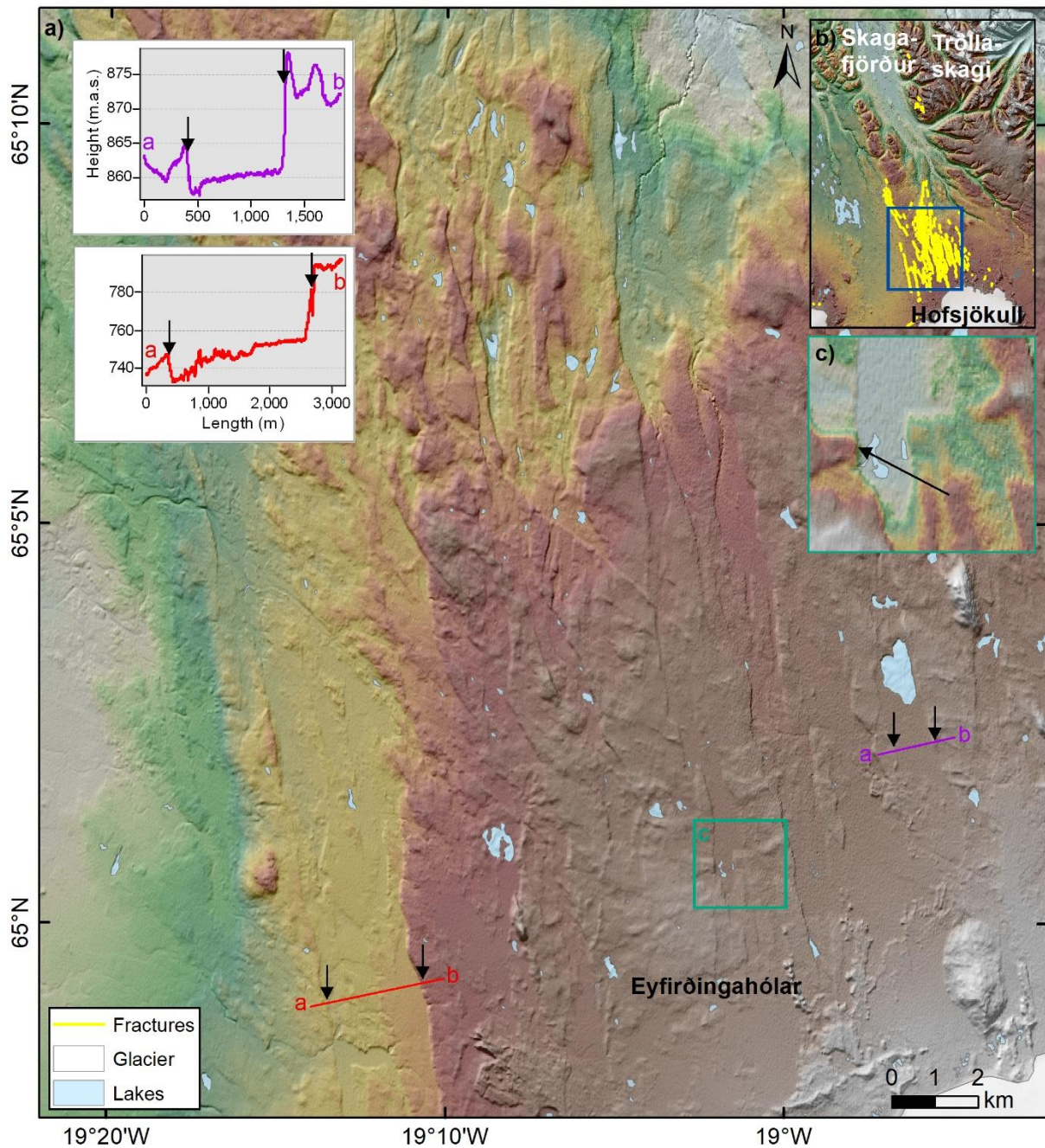
356 postglacial lava is from Hjartarson et al. (2019). ArcticDEM courtesy of the Polar Geospatial  
357 Center.



358

359 Fig. 12. Faults in the southern Hofsjökull fissure swarm. a) Fault in a hyaloclastite formation,  
360 with a throw of ~30 m. b) Fault in the postglacial Illahraun lava, with a throw of ~2 m. Páll  
361 Einarsson is sitting next to the Trimble Pathfinder ProXR GPS instrument.

362



363

364 Fig. 13. a) The northern Hofsjökull fissure swarm consists of multiple grabens and other faults.  
 365 b) The northern Hofsjökull fissure swarm. Blue frame indicates the location of a). c) Examples  
 366 of faults cutting glacial moraines, indicating that the faults have been active in postglacial times.  
 367 The location is shown in the green frame in a). Inset graphs show two examples of profiles  
 368 across grabens, the profiles are marked in a).

369

370

371



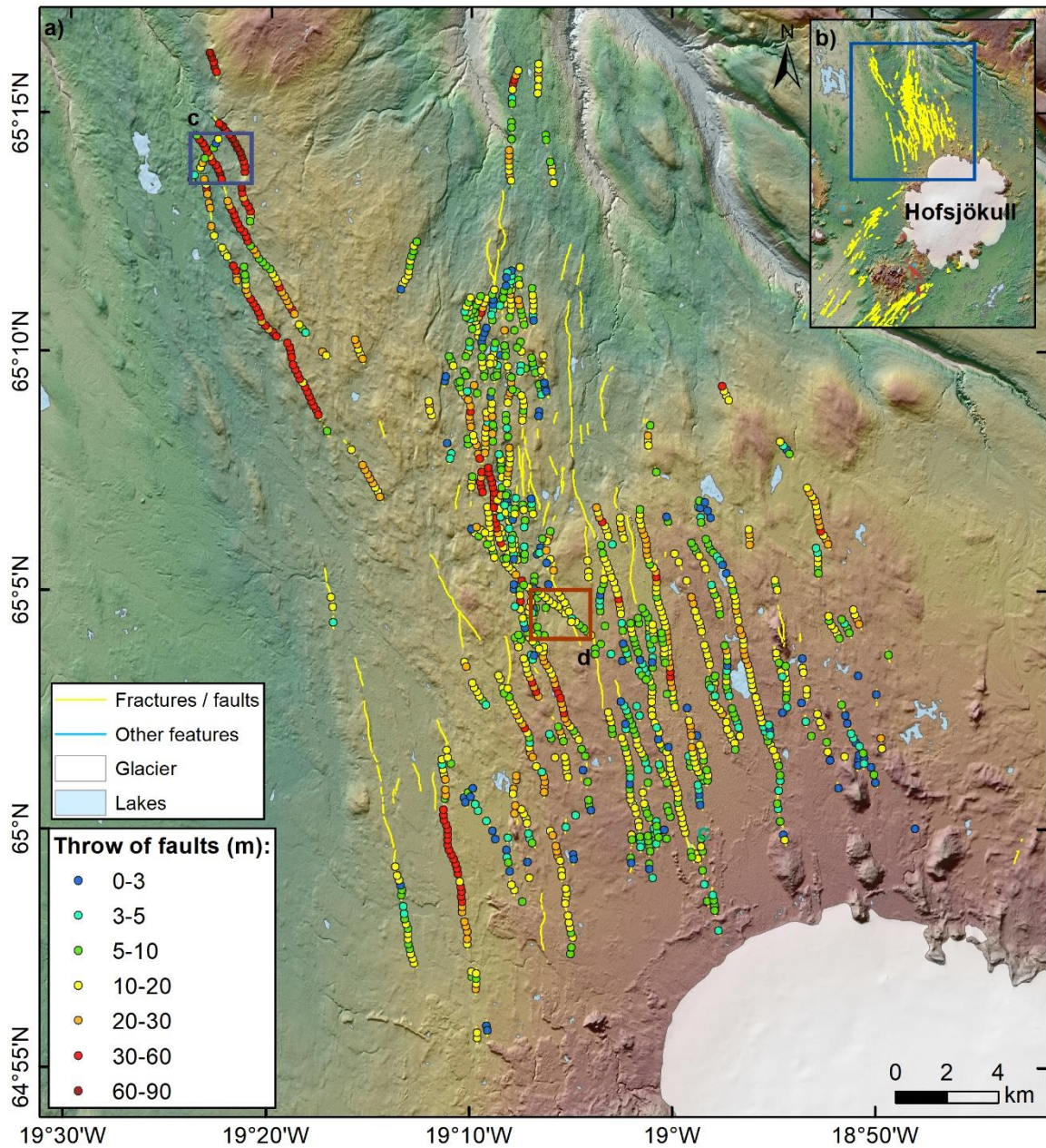
372 **5.4. The northern Hofsjökull fissure swarm:**

373 The northern Hofsjökull fissure swarm extends at least 40 km north of the Hofsjökull volcano  
374 (Fig. 3). However, freshly looking fractures can be found farther to the north, in the Tröllaskagi  
375 area by the northern coast of Iceland (Fig. 13). These fractures might be a separate entity not  
376 related to the northern Hofsjökull fissure swarm; the Tröllaskagi fractures will therefore not be  
377 discussed further in this paper.

378 The overall orientation of the northern Hofsjökull fissure swarm is towards the north-  
379 northwest. The orientation of individual fractures there is, however, more varied than in the  
380 fissure swarms extending to the south and west of the Hofsjökull glacier (Figs. 3 and 5). Three  
381 fracture population orientations are prevalent: A north-northwesterly orientation, which  
382 prevails in the southern and middle part of the fissure swarm, a northwesterly orientation which  
383 intermingles with the north-northwesterly oriented faults, and a northerly orientation which is  
384 mostly found in the northernmost part of the fissure swarm (Fig. 3).

385 Throws of faults in the northern Hofsjökull fissure swarm varies significantly. Although  
386 the faults in the main part of the fissure swarm generally have throws of less than 30 m, some  
387 faults, especially in the western part, have larger offsets (Figs. 14 and 15). This applies  
388 particularly to the northwesterly oriented population of faults located in the northwesternmost  
389 part of this area. This fault population is overprinted by the more northerly oriented faults which  
390 extend towards the Skagafjörður valley (Figs. 3 and 13). The northwesterly oriented faults  
391 generally have larger offsets than the northerly oriented fault population, even though they are  
392 in surface formations of a similar age (Jóhannesson and Sæmundsson, 1998a). Profiles across  
393 the northern Hofsjökull fissure swarm show that faults in the northern part of it are mainly  
394 downthrown towards the west (Fig. 15). This trend continues somewhat in the profiles further  
395 to the south, but there, profiles showing small grabens become more prevalent.

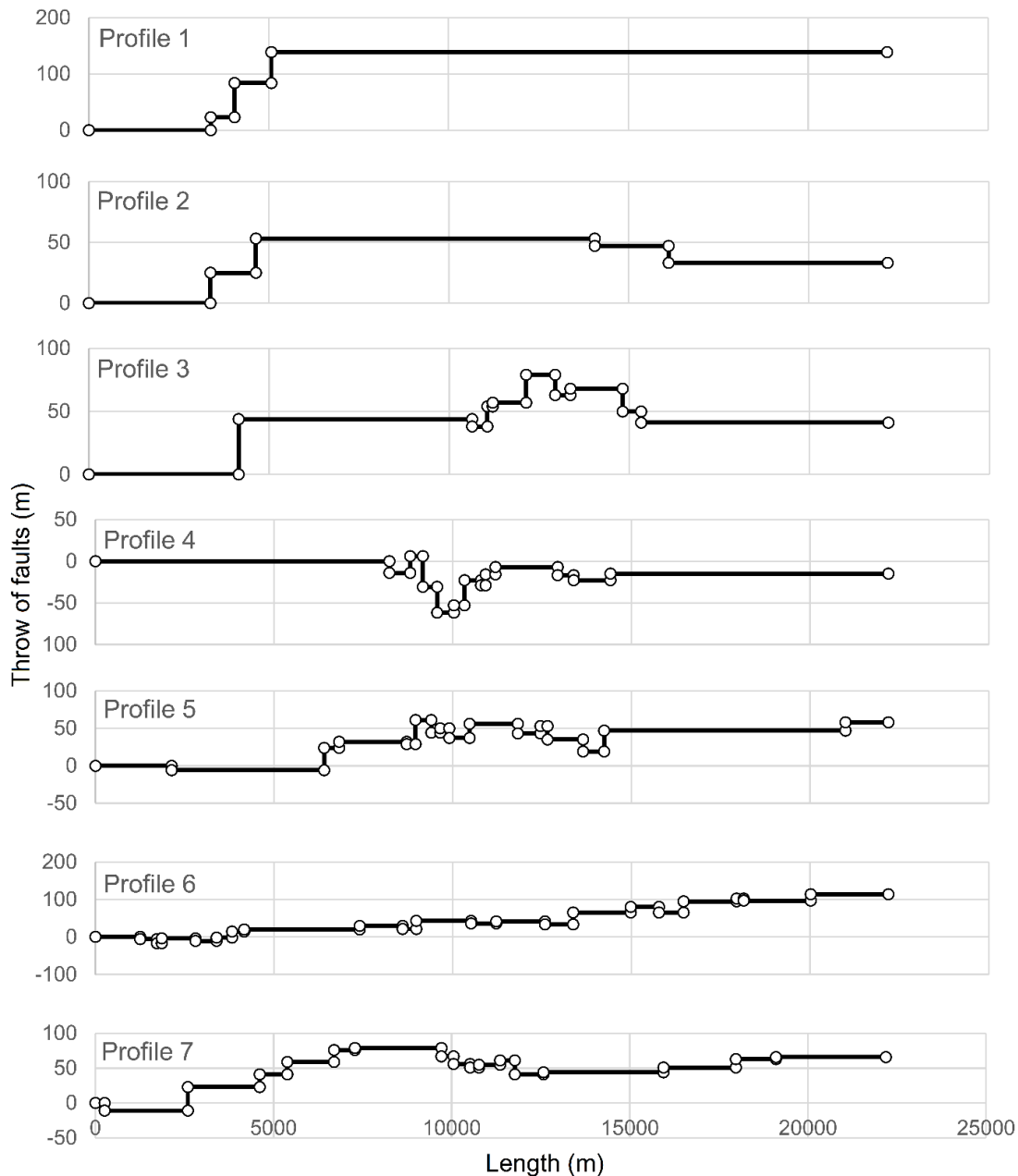
396 No clear sink holes were found in the northern Hofsjökull fissure swarm, which suggests  
397 that the fissure swarm has not been active for a considerable time, despite the significant throw  
398 of faults (Figs. 14-17). In addition, a fault in its southern part, near Eyfirðingahólar, is covered  
399 with unbroken hyaloclastite (Figs. 13 and 16). The hyaloclastite is from the last part of the last  
400 glaciation (Hjartarson et al., 2019). This indicates that the fault has not been active since the  
401 subglacial eruption which formed the hyaloclastite occurred.



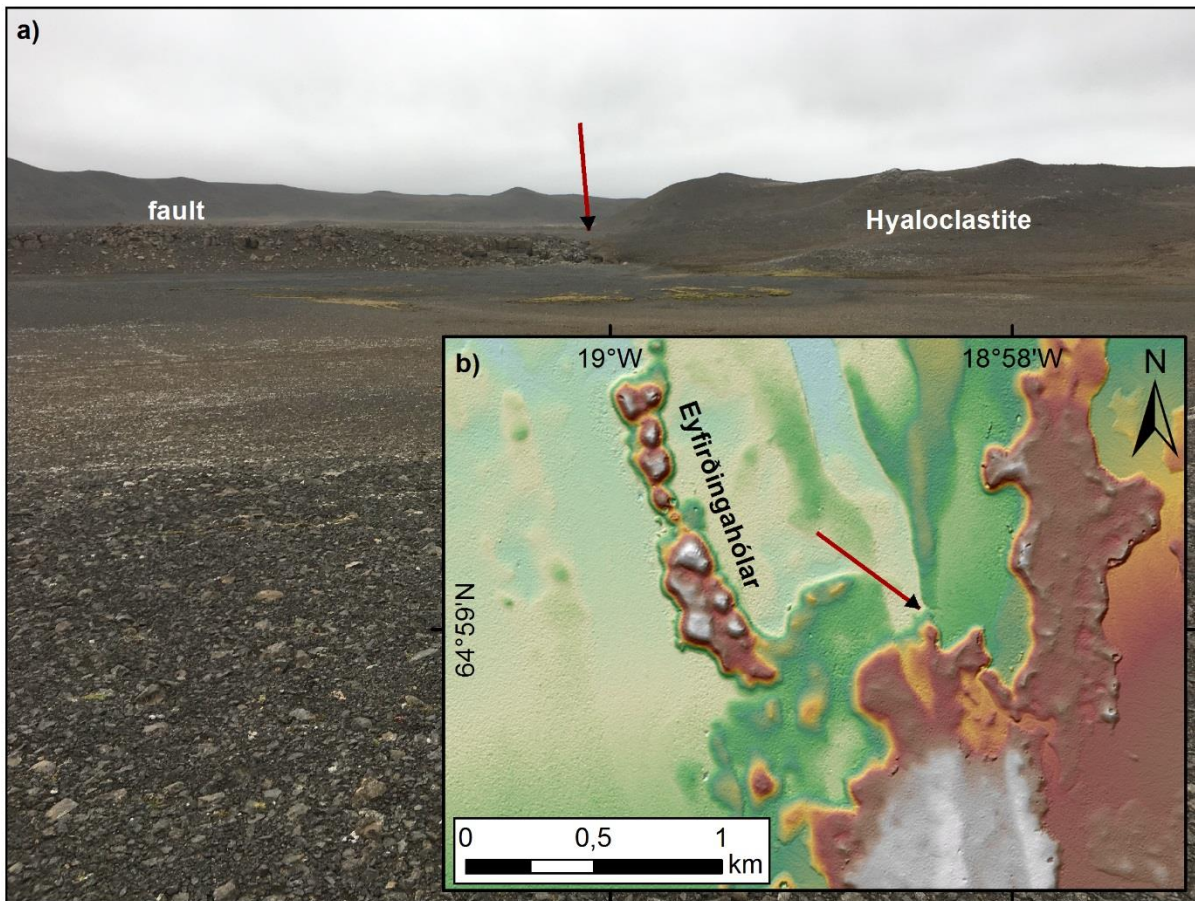
402

403

404 Fig. 14. a) Throw of faults in the northern Hofsjökull fissure swarm. Gaps in the measurements  
 405 are due to gaps in the ArcticDEMs. b) An overview map of the northern Hofsjökull fissure  
 406 swarm. c) An example of an aerial photograph showing faults, see a) for location. d) Another  
 407 example of an aerial photograph showing faults, see a) for location. The aerial photographs are  
 408 from Loftmyndir Corp.



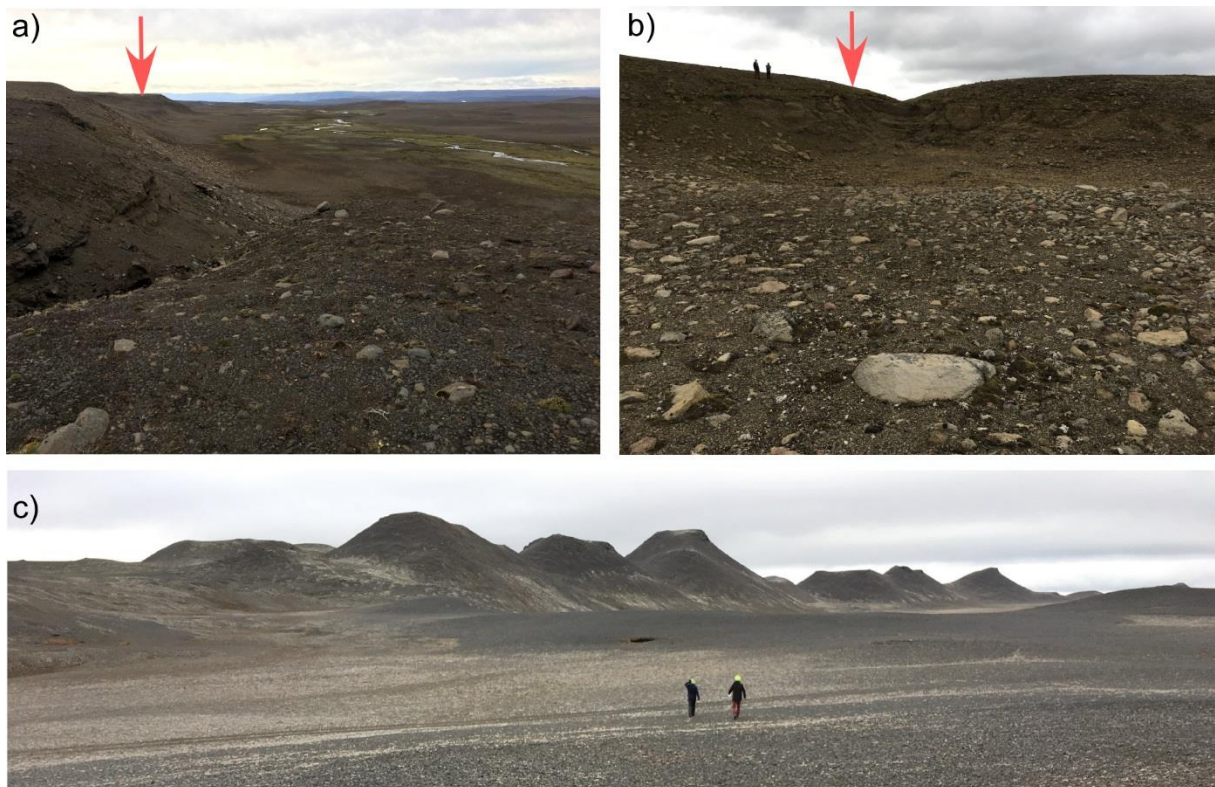
409  
 410 Fig. 15. Throw as a function of a distance along a profile across the northern Hofsjökull fissure  
 411 swarms, showing offset of faults. Negative values indicate downthrow towards the east. The  
 412 location of the profiles is shown in Fig. 3.



414 Fig. 16. a) A fault near Eyfirðingahólar. This fault is covered by an unbroken hyaloclastite,  
415 implying that the fault has not moved after the formation of the hyaloclastite. b) The location  
416 of the fault. c) A closer look at the boundary between the fault and the hyaloclastite. ArcticDEM  
417 courtesy of the Polar Geospatial Center.

418

419



420

421 Fig. 17. Fieldwork in the northern Hofsjökull fissure swarm. a) Fault in the central part of the  
422 northern HFS. Red arrow points to the fault. b) View towards another fault in the northern HFS,  
423 for scale, see two persons left of the red arrow. c) The Eyfirðingahólar pillow lava mounds.

424

## 425 6. Discussion

426 The mapping and analyzing of the fissure swarms of the Hofsjökull volcanic system indicate  
427 that they are mostly composed of grabens of various widths and depths, as indicated by the  
428 difference in the throw of faults (Figs. 3, 4, 6-10, 13, 15). The northwestern part of the northern  
429 Hofsjökull fissure swarm has a different appearance. There, most faults have a dip direction  
430 towards the west, often with a large-scale throw, and trend more northwestward than the more

431 northerly-oriented faults to the east of them (Figs. 3b, 14a and 15). They appear therefore to  
432 form a different fault population than the other faults in the northern Hofsjökull fissure swarm.

433

#### 434 6.1. Local stress field of the Hofsjökull central volcano vs. the regional stress field

435 Fissure swarms tend to radiate away from the Hofsjökull central volcano. This indicates that  
436 the Hofsjökull central volcano has a significant local stress field. This pattern is visible in the  
437 western Hofsjökull fissure swarm, where faults closest to the Hofsjökull central volcano bend  
438 more towards the northeast, while faults farther away have a more north-northeasterly  
439 orientation (Fig. 3). In addition, Holocene lava flows have been erupted not only north and  
440 south of the Hofsjökull central volcano, but also east and west of it (Hjartarson et al., 2019).  
441 This suggests that a local stress field of the Hofsjökull central volcano plays a significant role  
442 in this area, as it can cause the formation of a radial pattern of dike intrusions when  $\sigma_3$  follows  
443 a circular trace around the magma source in central volcanoes (e.g. Anderson, 1951;  
444 Nakamura, 1977)

445 Sometimes, fissure swarms in Iceland cut central volcanoes without much deviation of  
446 fracture orientations. This can indicate that the local stress field of the central volcano was not  
447 significant when the fractures within the fissure swarms formed, or that the principal axes of  
448 the regional stress field and the local stress field were aligned. This applies as an example to  
449 the Fremrinámar and Þeistareykir central volcanoes in the Northern Volcanic Zone in Iceland  
450 (Fig. 1a) (Hjartardóttir et al., 2016c; Magnúsdóttir and Brandsdóttir, 2011; Tibaldi et al.,  
451 2020). The Krafla central volcano has some local stress field, but mostly, the fractures follow  
452 the regional stress field (Hjartardóttir et al., 2012). Two central volcanoes in the Northern  
453 Volcanic Zone show significant local stress field. These are the Askja central volcano  
454 (Hjartardóttir et al., 2009), and the Bárðarbunga central volcano, where a dike intrusion,  
455 which occurred in 2014, started by propagating away from the Bárðarbunga central volcano in  
456 a southeasterly direction, far from the north-northeasterly direction expected if it would be  
457 opening perpendicular to the plate spreading direction in the area (DeMets et al., 1994;  
458 Sigmundsson et al., 2015). As the dike propagated away from the central volcano, it changed  
459 its heading until its distal part aligned with the regional stress field (Hjartardóttir et al., 2016b;  
460 Sigmundsson et al., 2015). This suggests that some central volcanoes in Iceland have a  
461 significant local stress field, and that the strength of the local stress field varies between  
462 central volcanoes. In the case of Hofsjökull, its local stress field may be dominant because it  
463 is not on the main plate boundary, therefore divergent plate movements are small or non-

464 existent in this area (Fig. 1). This local stress field may also be augmented by the close  
465 proximity of the Hofsjökull central volcano to the center of the Iceland hotspot, which is near  
466 the Bárðarbunga central volcano (Wolfe et al., 1997). It is also likely that strength of the local  
467 stress field of the central volcano can vary with time, depending on whether the magma  
468 source is inflating or not. Therefore, the relative contribution of the local stress field and the  
469 regional stress field can vary (e.g. Geshi, 2005; Magee et al., 2012). The eruptions on the east  
470 and west flanks of Hofsjökull could thus represent periods of a strong local stress field of the  
471 Hofsjökull central volcano, implying a significant inflation of the volcano at the time.

472

### 473 6.2. The orientation of fractures and faults in the northern Hofsjökull fissure swarm

474 The northern Hofsjökull fissure swarm is not located on a clear plate boundary (Fig. 1). Its  
475 NNW-orientation is also far from the NNE orientation which would be expected if the fissure  
476 swarm would open perpendicular to the plate spreading between the Eurasian and the North  
477 American plates.

478 It is therefore not clear why the Hofsjökull fissure swarm is oriented towards the  
479 NNW. One possibility is that the orientation of the fissure swarm is caused by differences in  
480 the crustal thickness in this area. Measurements of seismic velocities show that an area of  
481 increased crustal thickness extends in the NNW direction from the center of the Iceland  
482 hotspot near the Bárðarbunga central volcano, extending into the area where the northern  
483 Hofsjökull fissure swarm is located (Fig. 1a) (Allen, 1999; Brandsdóttir and Menke, 2008;  
484 Menke, 1999). West of this area, the crustal thickness decreases significantly. The NNW  
485 oriented Hofsjökull fissure swarm is therefore nearly parallel with the area of increased  
486 crustal thickness, and with the boundary between the thicker and the thinner crust.

487 During deglaciations, crustal blocks of different thicknesses can respond differently to  
488 the unloading of the glaciers. Therefore, crustal uplift can occur at different rates, causing  
489 enhanced differential stresses in a zone oriented parallel with the boundaries of these crustal  
490 blocks, i.e. in the NNW orientation in this case. In the absence of the crustal stresses by the  
491 divergent plate boundary, these divergent stresses may become the governing factor in where  
492 dike injections from the Hofsjökull central volcano propagate, therefore creating and  
493 maintaining the NNW orientation of the northern Hofsjökull fissure swarm.

494            Similar arguments have also been used to explain the Kerlingar fault at the eastern  
495 boundary of the Northern Volcanic Zone, which has also been active during the Holocene  
496 (Hjartardóttir et al., 2010). According to this suggestion, such differences in crustal thickness  
497 can cause dominant stress fields in areas where little or no deformation takes place due to  
498 plate divergence. This could also explain why fractures in the Northern Hofsjökull fissure  
499 swarm became activated by the end of the last glaciation, in the beginning of the Holocene,  
500 but has not been active recently, as observed by the lack of sink holes in the area.

501            The differently oriented fault populations in the northern Hofsjökull fissure swarm; the  
502 northerly fault system and the northwesterly fault system, suggest that the stress field has  
503 changed significantly. It is unclear why this occurred, but this might be explained by a  
504 changing stress field as the glacier retreated farther inland during the last deglaciation. Such  
505 an interaction between the orientation of dyke intrusions and crustal stresses due to uplift of  
506 land during glacier retreat has been used to explain the anomalous orientation of a recent dike  
507 intrusion in the Northern Volcanic Zone during small-scale glacier retreats at present time  
508 (Hooper et al., 2011), and this could also play a large part during large-scale glacier retreats as  
509 occurred during the end of the last glaciation.

510

511            *6.3. Activity of the Hofsjökull fissure swarms at the end of the last glaciation and during*  
512            *the Holocene*

513            Both the western and southern Hofsjökull fissure swarms include fractures and faults in  
514 Holocene lava flows. Therefore, it is clear that these fissure swarms have been active during  
515 postglacial times, the western fissure swarm sometime after the emplacement of the ~10.000  
516 years old Kjalhraun lava, and the southern fissure swarm sometime after the emplacement of  
517 the 4500-7000 years old Illahraun lava (Eason et al., 2015; Hjartarson et al., 2019).

518            The vertical movements of faults in these postglacial lava flows are, however, rather  
519 small, around 1-2 m in both. Vertical fault movements during individual dike intrusions are  
520 often around 1-3 m (or more) (e.g. Hjartardóttir et al., 2016b; Saemundsson, 1992;  
521 Sigurdsson, 1980; Wright et al., 2006). Therefore, it is possible that these fissure swarms  
522 have had only one dike intrusion each since the emplacement of these postglacial lava flows,  
523 or that some of the dike intrusions caused little surface deformation. If more dike intrusions  
524 have occurred during this time period they would most likely have propagated shorter



525 distances from the Hofsjökull central volcano, therefore not affecting the postglacial lava  
526 flows.

527 The postglacial lava flows north of Hofsjökull have not been fractured. They cover a very  
528 small part of the fissure swarm, and therefore, the fissure swarm may have been activated  
529 without causing fracturing in the postglacial lava flows. Other evidences also suggest that the  
530 northern fissure swarm has not been very active during the Holocene. Firstly, no sink holes  
531 are found along faults of the fissure swarm, indicating that all sink holes have been filled with  
532 sediments. Secondly, the unbroken hyaloclastite which covers the fault east of  
533 Eyfirðingahólar (Fig. 16), suggests that the fault has not been active after the emplacement of  
534 the hyaloclastite. No independent dating is available for the hyaloclastite, but the appearance  
535 of it suggests that it is from the last part of the last glaciation, since it hasn't been eroded  
536 (Hjartarson et al., 2019). The hyaloclastite formed under a glacier, but the fault not, which  
537 indicates that the extent of the glacier was only slightly larger than today. If the fault was  
538 activated during the magmatic event which formed the hyaloclastite, then that should have  
539 happened at the end of the last glaciation. The glacier extend was then only slightly larger  
540 than today, but soon retreated leaving little time to erode the fault.

541 Hyaloclastite from the end of the last glaciation is found across the entire northwestern  
542 boundary of the Hofsjökull glacier, and is found at up to 8 km distance from the glacier (Fig.  
543 1c) (Hjartarson et al., 2019). This suggests that there was a significant volcanic activity in the  
544 Hofsjökull volcanic system at the end of the last glaciation. In addition, faults in the northern  
545 Hofsjökull fissure swarm appear not to have been eroded significantly by a glacier. Also,  
546 faults cut glacial end moraines formed by the retreating glacier (Kaldal and Víkingsson,  
547 1990), showing that faulting has occurred after the glacier left the area (e.g. Fig. 13c). This  
548 pattern occurs on many different faults along the borders of different grabens. Therefore, it is  
549 likely that repeated dike intrusions occurred in the northern Hofsjökull fissure swarm at the  
550 end of the last glaciation or during the earliest part of Holocene, when glacier still covered the  
551 area closest to the current location of the Hofsjökull glacier. These repeated dike intrusions  
552 caused the tens of meters of throw along the many grabens which collectively define the  
553 northern Hofsjökull fissure swarm (e.g. Figs. 13 and 14). That would be in line with other  
554 evidences of increased volcanic activity in Iceland during that time period (e.g.  
555 Gudmundsson, 1986; Sigvaldason et al., 1992). Such an increase in magmatic activity,  
556 including eruptions and dike intrusions, can occur because of a rapid fall in pressure due to  
557 the deglaciation (Sigmundsson et al., 2010; Sigvaldason et al., 1992).

558

559 *6.4. The lack of fractures and faults in the Kerlingarfjöll rhyolitic massif*

560 Few fractures and faults were found in the rhyolitic Kerlingarfjöll massif, although fissure  
561 swarms extend far south both east and west of Kerlingarfjöll. The lack of fractures and faults  
562 just north of Kerlingarfjöll can be due to the proximity of the Hofsjökull glacier and sediments  
563 deposited by the glacier and its rivers. However, few fractures were also found in the  
564 Kerlingarfjöll massif itself as well as at the southern border of the Kerlingarfjöll rhyolitic  
565 massif, where the few faults which are found have small throws (Fig. 11). On the other hand,  
566 high density of fractures is found just east, west, and south of Kerlingarfjöll. Therefore, it  
567 appears that there is a “fissure swarm shadow” in the vicinity of the Kerlingarfjöll rhyolitic  
568 massif. This suggests that dike intrusions are hindered near Kerlingarfjöll. Either vertically fed  
569 dikes do not ascend high enough to cause surface deformation, or dikes fed horizontally from  
570 the Hofsjökull volcano do not penetrate through Kerlingarfjöll

571

572 Two processes might contribute to this “fissure swarm shadow”:

573 *1. Basaltic magma may have a hard time penetrating the lower density rhyolitic layers*  
574 *close to the surface*

575 Such hindering of basaltic dike intrusions can occur due to density differences between  
576 the lower density rhyolitic material closer to the surface and higher density basaltic dikes or  
577 sills. Basaltic magma is trapped and ponds at the level of neutral buoyancy instead of protruding  
578 up to the surface. Such mechanism has been used to explain the lack of basaltic formations in  
579 Yellowstone (USA), and in the Torfajökull caldera (Iceland) (Dzurisin et al., 1994;  
580 Sæmundsson, 2011; Walker, 1974).

581 The basaltic hyaloclastite formations in and near Kerlingarfjöll nevertheless indicate  
582 that basaltic magma does in some cases reach the surface (Fig. 1c), our suggestions are therefore  
583 more indicative on how “difficult” it is for the basaltic magma to reach the surface. This  
584 suggestion could explain why there is a high-temperature geothermal area in Kerlingarfjöll,  
585 even though the surface formations there are rather old. No volcanic activity is known in the  
586 Holocene, the rhyolites are between ~68 and 350 ka of age, and the hyaloclastite formations are  
587 from the early part of the Weichselian (Flude et al., 2010; Hjartarson et al., 2019). Basaltic dike

588 intrusions ponded under the rhyolitic massif, could cause uplift of the rhyolitic lava domes  
589 found in the area and lead to increased geothermal activity.

590

## 591 2. *The elevation of the Kerlingarfjöll rhyolitic massif*

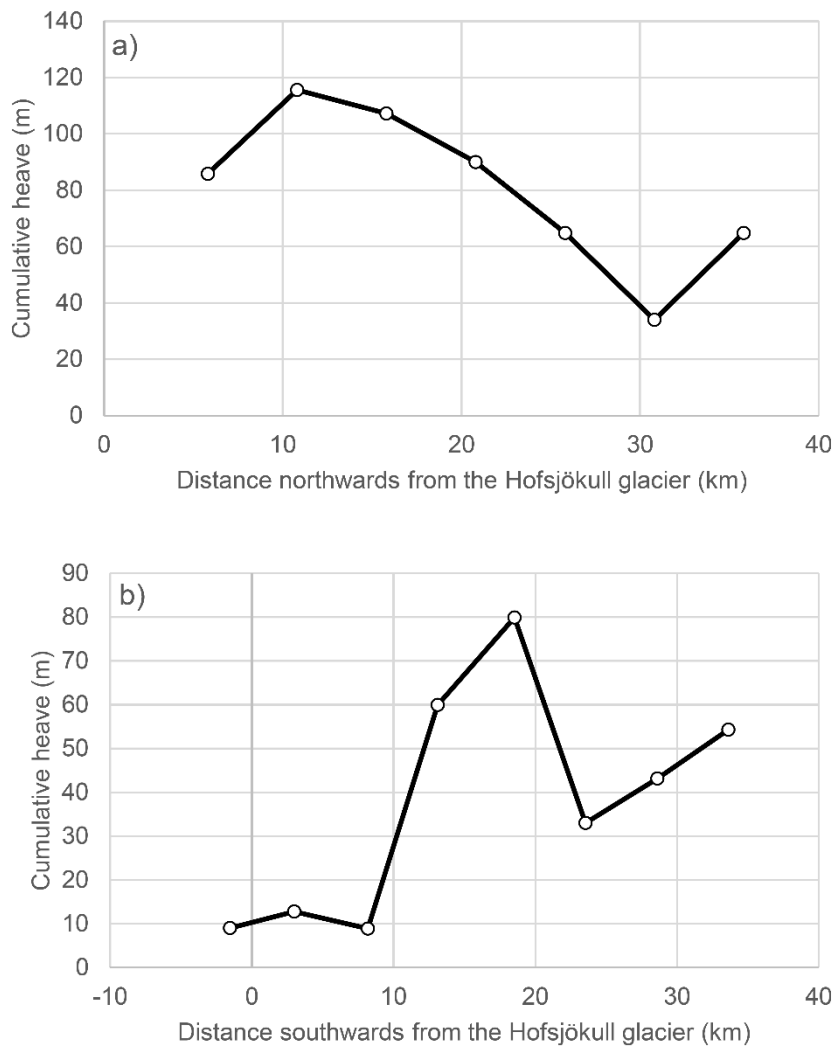
592 The distance from the top of dikes to the surface can increase near topographic highs, which  
593 would cause fewer fractures and grabens at the higher topographic elevations. Such an inverse  
594 relationship between the number of fractures and elevation of topographic highs has been  
595 observed in monogenetic basaltic lava shields in Iceland (Hjartardóttir and Einarsson, 2015).  
596 Similarly, dike intrusions in Iceland have been observed to propagate to lower areas, where  
597 they become shallower and fissure eruptions eventually take place, as occurred during the  
598 Bárðarbunga dike intrusion in 2014 (Sigmundsson et al., 2015). The Kerlingarfjöll massif  
599 rises to about 500-600 m above its surroundings, and thus, dike intrusions can be diverted to  
600 either pond beneath the Kerlingarfjöll massif or propagate laterally at deeper levels towards  
601 the north or south, rather than propagating as shallow dikes under the massif. This can occur  
602 regardless of whether the dikes propagate directly up from the mantle, or laterally from the  
603 Hofsjökull central volcano.

604

## 605 6.5 Cumulative extension across the Hofsjökull fissure swarms

606 By calculating cumulative heave across each profile in Figs. 7 and 15, the dilatation across the  
607 fissure swarms can be assessed (Fig. 18). Here, a fault dip of  $65^\circ$  is assumed. In the northern  
608 Hofsjökull fissure swarm, the cumulative heave generally decreases with increasing distance  
609 northwards from the Hofsjökull central volcano (Fig. 18). The pattern is more complicated in  
610 the southern part (Fig. 18). There, the heave peaks in the middle part whereas it tapers both  
611 towards the north and south. The tapering in the northern part can at least partly be due to the  
612 profile crossing a glacier (Fig. 3). The southern and the northern Hofsjökull fissure swarms  
613 are in different tectonic regimes. While the northern Hofsjökull fissure swarm propagates  
614 into the North-American plate, the southern fissure swarms extend into the Hreppar  
615 microplate and are therefore in-between the Western and Eastern Volcanic Zones (Fig. 1).  
616 This could cause complicated patterns of extension across the southern Hofsjökull fissure  
617 swarms, as the dilatation across the fissure swarm could be associated not only with distance

618 from the Hofsjökull central volcano, but also with the interplay between the Western and  
619 Eastern Volcanic Zones.

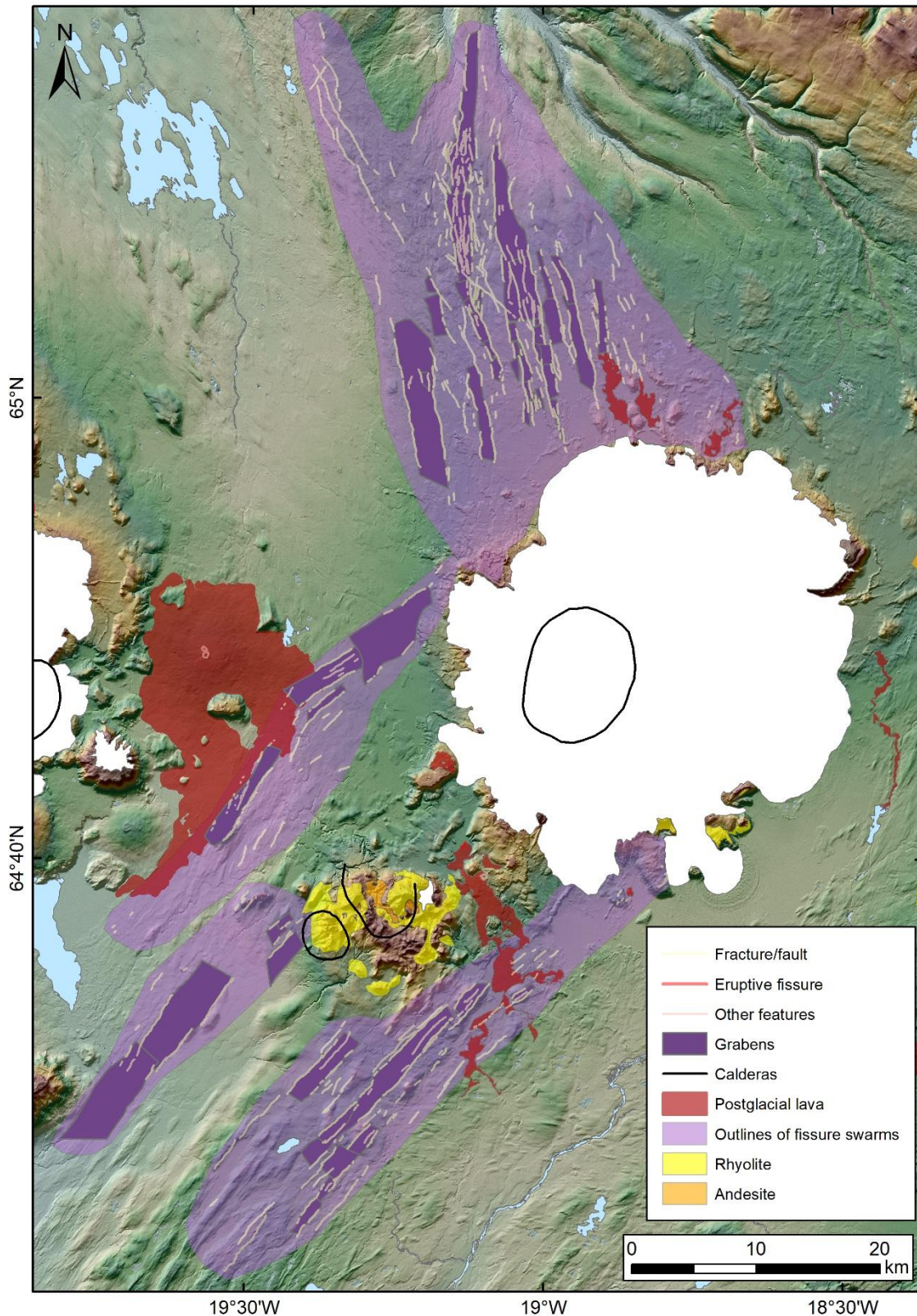


620

621 Fig. 18. The cumulative heave of faults with distance towards the north (a) and south (b) from  
622 the Hofsjökull glacier. The cumulative heave is calculated from the throw of faults in the  
623 profiles in Figs. 7 and 15, assuming that the faults have a dip of 65°.

624

625



626

627 Fig. 19. The overall structure of the Hofsjökull volcanic system, including grabens, faults, and  
 628 the outlines of the fissure swarms. Rhyolitic and andesitic formations were mapped by the  
 629 Iceland Geosurvey (ÍSOR) (Hjartarson et al., 2019). Postglacial lava flows were mapped by  
 630 ÍSOR and Sinton et al. (2005).

631 **Conclusions**

632 Our mapping of the fissure swarms of the Hofsjökull volcanic system reveals three to four  
633 separate swarms emanating from the central volcano, each one consisting of one to several  
634 parallel grabens (Fig. 19). The graben subsidence ranges from a few meters to more than 30 m,  
635 and the width from less than one to four km. The length of the swarms exceeds 50 km, measured  
636 from the caldera of the volcano. We interpret the grabens as the result of intrusion of shallow  
637 dikes from the central part of the system into the crust on both sides of the Central Iceland plate  
638 boundary. No Holocene eruptions are known with a source more than 20 km from the caldera.  
639 The Hofsjökull fissure swarms show that spreading rates have significant effect on the  
640 morphology and activity of fissure swarms. The lack of sink holes and other clear indicatives  
641 of most recent movements in the Hofsjökull fissure swarms indicates that they have been less  
642 active than the fissure swarms where full spreading rates are taking place, as an example in the  
643 Northern Volcanic Zone, Iceland. Faults in the postglacial Illahraun and Kjalhraun lavas on the  
644 other hand indicate that the southern fissure swarms have been activated during postglacial  
645 times.

646 The northwesterly orientation of the northern Hofsjökull fissure swarm is far from being  
647 perpendicular to the current plate spreading direction, indicating that the current spreading  
648 direction cannot explain the orientation. We suggest that the northwesterly orientated faults  
649 were formed and/or reactivated due to differential movements of crustal blocks of different  
650 thicknesses during the last deglaciation.

651 The lack of faults in the Kerlingarfjöll rhyolitic massif (Fig. 19), indicates that dikes  
652 have not propagated to shallow levels in that area, although faults and grabens east, west and  
653 south of Kerlingarfjöll suggest shallow dike intrusions there. We suggest that the lack of  
654 shallow dike intrusions under Kerlingarfjöll is due to a density barrier. Higher density basaltic  
655 dikes become trapped under lower density rhyolite. The basaltic intrusions under Kerlingarfjöll  
656 would thus be a heat source for the high-temperature geothermal area in Kerlingarfjöll despite  
657 the lack of recent eruptions. Another possible explanation for the lack of faults in Kerlingarfjöll  
658 is that Kerlingarfjöll is a topographic high, the distance to the top of a propagating dike will  
659 thus increase under Kerlingarfjöll, unless the dike propagates to higher elevations, which is  
660 unlikely.

661

662

## 663 **Acknowledgements**

664 We would like to thank Julia Annina Heilig, Sveinbjörn Steinþórsson and Kristján Haukdal  
665 Jónsson who assisted us during fieldwork in the Hofsjökull fissure swarms. We would also like  
666 to thank Kristján Sæmundsson and Magnús Á. Sigurgeirsson for fruitful discussions. The paper  
667 was improved significantly by response to comments by the editor and reviewers of this paper:  
668 Diana Roman, Craig Magee and an anonymous reviewer. The project is funded by the Icelandic  
669 Research Fund, grant number: 196226-052. Information on bedrock geology is from Iceland  
670 Geosurvey (ÍSOR). Aerial photographs are from Loftmyndir Corp. ArcticDEMs are provided  
671 by the Polar Geospatial Center under NSF-OPP awards 1043681, 1559691, and 1542736. The  
672 TanDEM-X digital elevation model is from the German Space Agency (DLR), under the project  
673 of IDEM\_GEOL0123. Cartographic data (outlines of glaciers, lakes, rivers) are from the IS50  
674 database of the National Land Survey of Iceland.

675

## 676 **References**

- 677 Allen, R.M., 1999. The mantle plume beneath Iceland and its intergration with the North Atlantic  
678 Ridge: A seismological investigation, Princeton University, Princeton, NJ, USA, 184 pp.
- 679 Anderson, E.M., 1951. The dynamics of faulting and dyke formation with applications to Britain.  
680 Hafner Pub. Co.
- 681 Árnadóttir, T., Lund, B., Jiang, W., Geirsson, H., Björnsson, H., Einarsson, P. and Sigurðsson, T., 2009.  
682 Glacial rebound and plate spreading: results from the first countrywide GPS observations in  
683 Iceland. *Geophys J Int*, 177(2): 691-716.
- 684 Björnsdóttir, T. and Einarsson, P., 2013. Evidence of recent fault movements in the Tungnafellsjökull  
685 fissure swarm in the Central Volcanic Zone, Iceland. *Jökull*, 63: 17-32.
- 686 Björnsson, H., 1986. Surface and bedrock topography of ice caps in Iceland, mapped by radio echo-  
687 sounding. *Annals of Glaciology*, 8: 11-18.
- 688 Björnsson, H., 1988. Hydrology of ice caps in volcanic regions. *Societas Scientarium Islandica*,  
689 University of Iceland.
- 690 Brandsdóttir, B. and Menke, W.H., 2008. The seismic structure of Iceland. *Jökull*, 58: 17-34.
- 691 DeMets, C., Gordon, R.G., Argus, D.F. and Stein, S., 1994. Effect of recent revisions to the  
692 geomagnetic reversal time-scale on estimates of current plate motions. *Geophys Res Lett*,  
693 21(20): 2191-2194.
- 694 Dumont, S., Sigmundsson, F., Parks, M.M., Drouin, V.J., Pedersen, G., Jónsdóttir, I., Höskuldsson, Á.,  
695 Hooper, A., Spaans, K., Bagnardi, M., Gudmundsson, M.T., Barsotti, S., Jónsdóttir, K.,  
696 Högnadóttir, T., Magnússon, E., Hjartardóttir, Á.R., Dürig, T., Rossi, C. and Oddsson, B., 2018.  
697 Integration of SAR Data Into Monitoring of the 2014–2015 Holuhraun Eruption, Iceland:  
698 Contribution of the Icelandic Volcanoes Supersite and the FutureVolc Projects. *Frontiers in*  
699 *Earth Science*, 6: 231.
- 700 Dzurisin, D., Yamashita, K.M. and Kleinman, J.W., 1994. Mechanisms of crustal uplift and subsidence  
701 at the Yellowstone caldera, Wyoming. *Bull Volcanol*, 56(4): 261-270.
- 702 Eason, D.E., Sinton, J.M., Grönvold, K. and Kurz, M.D., 2015. Effects of deglaciation on the petrology  
703 and eruptive history of the Western Volcanic Zone, Iceland. *Bull Volcanol*, 77(6): 1-27.

704 Einarsson, P., 1991. Earthquakes and present-day tectonism in Iceland. *Tectonophysics*, 189(1-4):  
705 261-279.

706 Einarsson, P., 2008. Plate boundaries, rifts and transforms in Iceland. *Jökull*, 58: 35-58.

707 Einarsson, P. and Brandsdóttir, B., 2021. Seismicity of the Northern Volcanic Zone of Iceland.  
708 *Frontiers in Earth Science*, 9: 166.

709 Einarsson, P. and Sæmundsson, K., 1987. Earthquake epicenters 1982-1985 and volcanic systems in  
710 Iceland (map). In: Þ.I. Sigfússon (Editor), *Í hlutarins eðli*, Festschrift for Þorbjörn  
711 Sigurgeirsson. Menningarsjóður, Reykjavík.

712 Flude, S., McGarvie, D.W., Burgess, R. and Tindle, A.G., 2010. Rhyolites at Kerlingarfjöll, Iceland: the  
713 evolution and lifespan of silicic central volcanoes. *Bull Volcanol*, 72(5): 523-538.

714 Geshi, N., 2005. Structural development of dike swarms controlled by the change of magma supply  
715 rate: the cone sheets and parallel dike swarms of the Miocene Otoge igneous complex,  
716 Central Japan. *J Volcanol Geotherm Res*, 141(3-4): 267-281.

717 Grönvold, K., 1972. Structural and petrochemical studies in the Kerlingarfjöll region, southwest  
718 Iceland. Oxford Univ., Ph. D. diss.

719 Gudmundsson, A., 1986. Mechanical aspects of postglacial volcanism and tectonics of the Reykjanes  
720 Peninsula, southwest Iceland. *Journal of Geophysical Research: Solid Earth*, 91(B12): 12711-  
721 12721.

722 Helmens, K.F., 2014. The Last Interglacial–Glacial cycle (MIS 5–2) re-examined based on long proxy  
723 records from central and northern Europe. *Quaternary Science Reviews*, 86: 115-143.

724 Hjartardóttir, Á.R. and Einarsson, P., 2015. The interaction of fissure swarms and monogenetic lava  
725 shields in the rift zones of Iceland. *J Volcanol Geotherm Res*, 299: 91-102.

726 Hjartardóttir, Á.R., Einarsson, P. and Björgvinsdóttir, S., 2016a. Fissure swarms and fracture systems  
727 within the Western Volcanic Zone, Iceland – effects of spreading rates. *J Struct Geol*, 91: 39-  
728 53.

729 Hjartardóttir, Á.R., Einarsson, P., Bramham, E. and Wright, T.J., 2012. The Krafla fissure swarm,  
730 Iceland and its formation by rifting events. *Bull. Volcanol.*, 74(9): 2139-2153.

731 Hjartardóttir, Á.R., Einarsson, P. and Brandsdóttir, B., 2010. The Kerlingar fault, Northeast Iceland: A  
732 Holocene normal fault east of the divergent plate boundary. *Jökull*, 60: 103-116.

733 Hjartardóttir, Á.R., Einarsson, P., Gudmundsson, M.T. and Högnadóttir, T., 2016b. Fracture  
734 movements and graben subsidence during the 2014 Bárðarbunga dike intrusion in Iceland. *J*  
735 *Volcanol Geotherm Res*, 310: 242-252.

736 Hjartardóttir, Á.R., Einarsson, P., Magnúsdóttir, S., Björnsdóttir, Þ. and Brandsdóttir, B., 2016c.  
737 Fracture systems of the Northern Volcanic Rift Zone, Iceland - an onshore part of the Mid-  
738 Atlantic plate boundary. In: T.J. Wright, A. Ayele, D.J. Ferguson, T. Kidane and C. Vye-Brown  
739 (Editors), *Magmatic Rifting and Active Volcanism*. The Geological Society of London, pp. 297-  
740 314.

741 Hjartardóttir, Á.R., Einarsson, P. and Sigurðsson, H., 2009. The fissure swarm of the Askja volcanic  
742 system along the divergent plate boundary of N Iceland. *Bull Volcanol*, 71(9): 961-975.

743 Hjartardóttir, Á.R., Hjaltadóttir, S., Einarsson, P., Vogfjörð, K. and Muñoz-Cobo Belart, J., 2015.  
744 Fracturing and earthquake activity within the Prestahnúkur fissure swarm in the Western  
745 Volcanic Rift Zone of Iceland. *J Geophys Res*, 120(12): 8743-8757.

746 Hjartarson, Á., Kaldal, I., Sæmundsson, K., Sigurgeirsson, M.Á. and Víkingsson, S., 2019. Jarðfræðikort  
747 af Mið-Íslandi 1:100 000. Íslenskar Orkurannsóknir, Landsvirkjun, Umhverfis og  
748 auðlindaráðuneytið, Reykjavík.

749 Hooper, A., Ófeigsson, B., Sigmundsson, F., Lund, B., Einarsson, P., Geirsson, H. and Sturkell, E., 2011.  
750 Increased capture of magma in the crust promoted by ice-cap retreat in Iceland. *Nat. Geosci.*,  
751 4(11): 783-786.

752 Jakobsdóttir, S.S., 2008. Seismicity in Iceland: 1994-2007. *Jökull*, 58: 75-100.

753 Jóhannesson, H. and Sæmundsson, K., 1998a. Geological map of Iceland. Bedrock geology. Icelandic  
754 Inst Natur Hist, Reykjavík.



755 Jóhannesson, H. and Sæmundsson, K., 1998b. Geological map of Iceland. Tectonics. Icelandic Inst  
756 Natur Hist, Reykjavík.

757 Kaldal, I. and Víkingsson, S., 1990. Early Holocene deglaciation in Central Iceland. *Jökull*, 40: 51-66.

758 Khodayar, M., Björnsson, S., Víkingsson, S. and Jónsdóttir, G.S., 2020. Unstable Rifts, a Leaky  
759 Transform Zone and a Microplate: Analogues from South Iceland. *Open Journal of Geology*,  
760 10(4): 317-367.

761 LaFemina, P.C., Dixon, T.H., Malservisi, R., Árnadóttir, Þ., Sturkell, E., Sigmundsson, F. and Einarsson,  
762 P., 2005. Geodetic GPS measurements in south Iceland: Strain accumulation and partitioning  
763 in a propagating ridge system. *J Geophys Res*, 110(B11): B11405.

764 Magee, C., Stevenson, C., O'driscoll, B., Schofield, N. and McDermott, K., 2012. An alternative  
765 emplacement model for the classic Ardnamurchan cone sheet swarm, NW Scotland,  
766 involving lateral magma supply via regional dykes. *J Struct Geol*, 43: 73-91.

767 Magnúsdóttir, S. and Brandsdóttir, B., 2011. Tectonics of the Þeistareykir fissure swarm. *Jökull*, 61:  
768 65-79.

769 Menke, W., 1999. Crustal isostasy indicates anomalous densities beneath Iceland. *Geophys Res Lett*,  
770 26(9): 1215-1218.

771 Nakamura, K., 1977. Volcanoes as possible indicators of tectonic stress orientation — principle and  
772 proposal. *J Volcanol Geotherm Res*, 2(1): 1-16.

773 Óladóttir, B.A., Sigmarsson, O., Larsen, G. and Devidal, J.-L., 2011. Provenance of basaltic tephra from  
774 Vatnajökull subglacial volcanoes, Iceland, as determined by major-and trace-element  
775 analyses. *The Holocene*: 0959683611400456.

776 Pollard, D.D., Delaney, P.T., Duffield, W.A., Endo, E.T. and Okamura, A.T., 1983. Surface deformation  
777 in volcanic rift zones. *Tectonophysics*, 94(1): 541-584.

778 Porter, C., Morin, P., Howat, I., Noh, M.-J., Bates, B., Peterman, K., Keeseey, S., Schlenk, M., Gardiner,  
779 J., Tomko, K., Willis, M., Kelleher, C., Cloutier, M., Husby, E., Foga, S., Nakamura, H., Platson,  
780 M., Wethington, M.J., Williamson, C., Bauer, G., Enos, J., Arnold, G., Kramer, W., Becker, P.,  
781 Doshi, A., D'Souza, C., Cummins, P., Laurier, F. and Bojesen, M., 2018. ArcticDEM. Harvard  
782 Dataverse.

783 Rubin, A.M. and Pollard, D.D., 1988. Dike-induced faulting in rift zones of Iceland and Afar. *Geology*,  
784 16(5): 413-417.

785 Sæmundsson, K., 1978. Fissure swarms and central volcanoes of the neovolcanic zones of Iceland. In:  
786 D.R. Bowes and B.E. Leake (Editors), *Crustal evolution in northwestern Britain and adjacent*  
787 *regions*. Seel House Press, Liverpool, England, pp. 415-432.

788 Sæmundsson, K., 2011. Torfajökull, Iceland – A rhyolite volcano and its geothermal resource,  
789 *Exploration for Geothermal Resources, Lake Bogoria and Lake Naivasha, Kenya*, pp. 1-11.

790 Sæmundsson, K., 1992. Geology of the Thingvallavatn area. *Oikos*, 64(1-2): 40-68.

791 Sigmundsson, F., 2006. Magma does the splits. *Nature*, 442(7100): 251-252.

792 Sigmundsson, F., Einarsson, P., Hjartardóttir, Á.R., Drouin, V., Jónsdóttir, K., Árnadóttir, T., Geirsson,  
793 H., Hreinsdóttir, S., Li, S. and Ófeigsson, B.G., 2020. Geodynamics of Iceland and the  
794 signatures of plate spreading. *J Volcanol Geotherm Res*, 391: 106436.

795 Sigmundsson, F., Hooper, A., Hreinsdóttir, S., Vogfjörð, K.S., Ófeigsson, B.G., Heimisson, E.R.,  
796 Dumont, S., Parks, M., Spaans, K., Gudmundsson, G.B., Drouin, V., Arnadóttir, T., Jonsdóttir,  
797 K., Gudmundsson, M.T., Hognadóttir, T., Fridriksdóttir, H.M., Hensch, M., Einarsson, P.,  
798 Magnusson, E., Samsonov, S., Brandsdóttir, B., White, R.S., Agustsdóttir, T., Greenfield, T.,  
799 Green, R.G., Hjartardóttir, A.R., Pedersen, R., Bennett, R.A., Geirsson, H., La Femina, P.C.,  
800 Björnsson, H., Pálsson, F., Sturkell, E., Bean, C.J., Mollhoff, M., Braidon, A.K. and Eibl, E.P.S.,  
801 2015. Segmented lateral dyke growth in a rifting event at Bardarbunga volcanic system,  
802 Iceland. *Nature*, 517(7533): 191-195.

803 Sigmundsson, F., Pinel, V., Lund, B., Albino, F., Pagli, C., Geirsson, H. and Sturkell, E., 2010. Climate  
804 effects on volcanism: influence on magmatic systems of loading and unloading from ice mass  
805 variations, with examples from Iceland. *Philosophical Transactions of the Royal Society A:*  
806 *Mathematical, Physical and Engineering Sciences*, 368(1919): 2519-2534.

807 Sigurdsson, O., 1980. Surface deformation of the Krafla fissure swarm in two rifting events. *Journal of*  
808 *Geophysics-Zeitschrift Fur Geophysik*, 47(1-3): 154-159.

809 Sigvaldason, G.E., Annertz, K. and Nilsson, M., 1992. Effect of glacier loading deloading on volcanism -  
810 postglacial volcanic production-rate of the Dyngjufjöll area, central Iceland. *Bull Volcanol*,  
811 54(5): 385-392.

812 Sinton, J., Grönvold, K. and Sæmundsson, K., 2005. Postglacial eruptive history of the Western  
813 Volcanic Zone, Iceland. *Geochem. Geophys. Geosyst.*, 6(12): Q12009.

814 Stevenson, J.A., Smellie, J.L., McGarvie, D.W., Gilbert, J.S. and Cameron, B.I., 2009. Subglacial  
815 intermediate volcanism at Kerlingarfjöll, Iceland: magma–water interactions beneath thick  
816 ice. *J Volcanol Geotherm Res*, 185(4): 337-351.

817 Tibaldi, A., Bonali, F.L., Mariotto, F.P., Corti, N., Russo, E., Einarsson, P. and Hjartardóttir, Á.R., 2020.  
818 Rifting kinematics produced by magmatic and tectonic stresses in the North Volcanic Zone,  
819 Iceland. *Frontiers in Earth Science*, 8: 174.

820 Torfason, H., 2003. Jarðhitakort af Íslandi og gagnasafn um jarðhita. Orkustofnun.

821 Tryggvason, E., 1984. Widening of the Krafla fissure swarm during the 1975–1981 volcano-tectonic  
822 episode. *Bull Volcanol*, 47(1): 47-69.

823 Valsson, G., Sigurðsson, T., Völksen, C. and Rennen, M., 2007. ISNET2004. Results from a resurvey of  
824 the Icelandic geodetic reference network (in Icelandic with an English summary), The  
825 National Land Survey of Iceland.

826 Walker, G.P., 1974. Eruptive mechanisms in Iceland. In: L. Kristjánsson (Editor), *Geodynamics of*  
827 *Iceland and the North Atlantic area*. Springer, pp. 189-201.

828 Wolfe, C.J., Bjarnason, I.T., VanDecar, J.C. and Solomon, S.C., 1997. Seismic structure of the Iceland  
829 mantle plume. *Nature*, 385(6613): 245-247.

830 Wright, T.J., Ebinger, C., Biggs, J., Ayele, A., Yirgu, G., Keir, D. and Stork, A., 2006. Magma-maintained  
831 rift segmentation at continental rupture in the 2005 Afar dyking episode. *Nature*, 442(7100):  
832 291-294.

833